

## Fast ejecta during the ascending phase of solar cycle 23: ACE observations, 1998–1999

L. F. Burlaga,<sup>1</sup> R. M. Skoug,<sup>2</sup> C. W. Smith,<sup>3</sup> D. F. Webb,<sup>4</sup>  
T. H. Zurbuchen,<sup>5</sup> and Alysha Reinard<sup>5</sup>

**Abstract.** We discuss fast ejecta observed at 1 AU during a period of increasing solar activity from February 5, 1998, to November 29, 1999. “Fast ejecta” are transient, noncorotating flows that move past the Earth during a day or more, with a maximum speed  $>600 \text{ km s}^{-1}$ . We identify two classes of fast ejecta at 1 AU: (1) magnetic clouds, whose local magnetic structure is that of a flux rope; and (2) “complex ejecta,” which are not flux ropes and have disordered magnetic fields. Nearly equal numbers of magnetic clouds and complex ejecta were found: four and five, respectively. The complex ejecta had weaker magnetic fields and higher proton temperatures than the magnetic clouds on average. The average  $\beta$  for the complex ejecta ( $0.25 \pm 0.09$ ) was larger than that for the magnetic clouds ( $0.06 \pm 0.04$ ). The complex ejecta and magnetic clouds had comparable speeds on average, namely,  $558 \pm 80$  and  $500 \pm 63 \text{ km s}^{-1}$ , respectively. Using the duration of the stream and that of the counterstreaming electrons to measure the ejecta, the average time for the complex ejecta to move past ACE was 3 days, which is more than twice that for the magnetic clouds. All of the magnetic clouds contain some material with a high  $\alpha$ /proton density ratio ( $>8\%$ ) and a density ratio of  $\text{O}^{7+}/\text{O}^{6+} > 1$ . However, three of the five complex ejecta did not contain material with  $\text{O}^{7+}/\text{O}^{6+} > 1$ , although four of the complex ejecta contained material with  $\text{O}^{7+}/\text{O}^{6+} > 1$ . All of the magnetic clouds caused geomagnetic storms. Three complex ejecta produced no geomagnetic storms. The other two complex ejecta produced geomagnetic storms indirectly: one by driving a shock into the rear of a magnetic cloud and the other by amplifying southward fields in its leading edge and interaction region. Most of the magnetic clouds were associated with a single solar source, but nearly all of the complex ejecta could have had multiple sources. We find evidence in the solar observations that some of the complex ejecta could have been produced by the interaction of two or more coronal mass ejections (CMEs). At least three CMEs might have interacted to produce a large complex ejection that arrived at 1 AU on May 4, 1998. This complex ejection was overtaking and interacting with a magnetic cloud. We discuss several hypotheses concerning the structures and origins of complex ejecta, including the likely possibility that some complex ejecta are formed by a series of interacting CMEs of various sizes.

### 1. Introduction

The existence of certain volumes of plasma moving at high speeds from the Sun to Earth was postulated to explain intense geomagnetic storms. For discussions of the early ideas about these flows, see the work of Lindeman [1919], Cocconi *et al.* [1958], Morrison [1956], Newton [1943], Chapman [1964], Chapman and Bartels [1940], and Akasofu and Chapman [1972]. Prior to the space age these flows were called clouds, plasma clouds, turbulent clouds, nascent streams, flare

streams, magnetic tongues, jets, magnetized plasma clouds, bottles, and bubbles. In publications based on in situ measurements such flows have been called postshock flows, drivers, transients, plasma clouds, flare ejecta, coronal mass ejections (CMEs), interplanetary CMEs (ICMEs), ejecta, and magnetic clouds. In accordance with the American Geophysical Union (AGU) index set, we use the term “ejecta” for such interplanetary flows and “CME” for coronal mass ejections (meaning mass ejections that can be seen moving through the corona with a coronagraph).

We identify “fast ejecta” operationally as transient, noncorotating flows that move past a point at 1 AU during a day or more and have a maximum speed  $>600 \text{ km s}^{-1}$ . A corotating flow is readily recognized by its high temperatures, low densities, and a stream interface at the leading edge. This paper discusses only “fast ejecta” because there is no unambiguous way to identify slow ejecta. Various signatures of ejecta are summarized by Zwickl *et al.* [1983], Gosling [1990, 1997], and Neugebauer and Goldstein [1997], but these signatures are not definitive. Gosling *et al.* [1973], Richardson and Cane [1995], and Cane *et al.* [1996] used low proton temperature  $T$  as a defining characteristic of ejecta, but low  $T$  can be found in the

<sup>1</sup>Laboratory for Extraterrestrial Physics, NASA Goddard Space Flight Center, Greenbelt, Maryland.

<sup>2</sup>Los Alamos National Laboratory, Los Alamos, New Mexico.

<sup>3</sup>Bartol Research Institute, University of Delaware, Newark, Delaware.

<sup>4</sup>Institute for Scientific Research, Boston College, Chestnut Hill, Massachusetts.

<sup>5</sup>Department of Atmospheric, Oceanic, and Space Sciences, University of Michigan, Ann Arbor, Michigan.

heliospheric plasma sheet in the absence of ejecta, and ejecta with high  $T$  do exist [Gosling *et al.*, 1987; Gosling, 1990; Richardson *et al.*, 1997].

During the sixties and seventies, many observations of ejecta were made, and there is a large literature on these events. However, those observations suggested that the magnetic field in ejecta is always disordered [Hundhausen, 1972], as conjectured by Morrison [1956]. Magnetic clouds (ejecta in which the magnetic field direction rotates smoothly through a large angle across the structure, the magnetic field strength is larger than average, and the proton temperature and  $\beta$  are relatively low) were identified by Burlaga *et al.* [1981, 1990] and interpreted as large magnetic loops with possibly helical magnetic field lines. Magnetic clouds are related to the early ideas of tongues, bubbles, and bottles with ordered magnetic fields, but we now understand that the basic magnetic structure is a flux rope, which was not considered in the early work. For reviews of the literature on magnetic clouds, see the work of Burlaga [1984, 1991, 1995] and Osherovich and Burlaga [1997].

Since magnetic clouds can be identified relatively unambiguously, one can divide a set of fast ejecta into two subsets, the fast magnetic clouds and the remaining subset that we call fast “complex ejecta.” The complex ejecta have a variety of signatures and forms, but all have variable magnetic field directions. It is possible that more than one model and one source must be invoked to account for the variety of complex ejecta, as discussed in section 9.

## 2. Selection of Events and Their Rate of Occurrence

We examined the ACE plasma and magnetic field data from February 5, 1998, to November 29, 1999, during the ascending phase of solar cycle 23. Streams with a duration  $>1$  day and with a maximum speed  $\geq 600$  km s $^{-1}$  were identified. Corotating streams, identified by a stream interface followed by a flow with relatively high temperature and low density, were eliminated. The remaining flows are the fast ejecta that we study below. We do not consider the slower ejecta. However, a number of magnetic clouds and noncloud ejecta with  $V_{\max} < 600$  km s $^{-1}$  were present. We found nine fast ejecta in the 298-day interval. Since the data were essentially continuous during the interval of 1.8 years under consideration, the rate of fast ejecta is 5 per year, or 0.4 per month.

Four of the ejecta that we selected were magnetic clouds, identified independently by Wind and ACE investigators. The other five ejecta are “complex ejecta,” which are simply fast ejecta lacking the signatures of magnetic clouds, as discussed above. As we shall show, the complex ejecta do not all have the same signature. Various estimates of the ratio of magnetic clouds to the total number of ejecta have been given. Klein and Burlaga [1982] found that over a solar cycle, magnetic clouds were observed at an average rate of 0.5–1 per month. Gosling *et al.* [1992] suggested that magnetic clouds represent one third of all ejecta. Cane *et al.* [1997] found a ratio of 50% on average. In our study of nine fast ejecta during the ascending phase of the current cycle, the magnetic clouds comprised nearly half ( $4/9 = 44\%$ ) of the fast ejecta.

## 3. Identification of Boundaries and Passage Times of Ejecta

No unambiguous signature of the boundaries of ejecta has been found, despite many attempts to find such signatures [see,

e.g., Burlaga, 1995, chap. 6; Neugebauer and Goldstein, 1997]. One needs to know the times of the boundaries in order to estimate the “passage time” of the ejecta (the time interval between the observation of the front boundary and the rear boundary by a spacecraft), the “length scale” (the passage time divided by the mean speed) of the ejecta, and the travel time from the solar source. However, distinct boundaries of ejecta might not always exist, particularly for complex ejecta.

In the case of magnetic clouds the front boundary is usually identified by an increase in the magnetic field strength, a large change in the magnetic field direction, and an abrupt drop in proton temperature. In some cases there may also be a magnetic hole and/or change in density at the front boundary. The rear boundary of a magnetic cloud is often more difficult to identify, but an increase in temperature and the end of a smooth rotation of the magnetic field direction during the passage of a magnetic cloud are often taken as signatures of the boundary. When the magnetic field is modeled as a force-free field configuration, various choices for the boundaries give different qualities of the fit, and the boundaries may be chosen as those that give the best fit. Despite the ambiguities, the various methods for identifying magnetic cloud boundaries generally give passage times that are consistent within  $\sim 10\%$ .

The boundaries of complex ejecta are very difficult to identify. It is likely that thin boundaries do not exist in general; instead, there might often be a broad, turbulent transition at the front, such as that observed in gas from an explosion, and a tail or wake on the back side. We shall see that the temperature and the magnetic field strength can be either high or low in complex ejecta, so that one cannot use these fields to identify the boundaries. The presence of increased helium abundance relative to protons, unusual charge states, and bidirectional anisotropies in energetic electrons and protons are strong evidence for the presence of ejecta [Zwickl *et al.*, 1983], but these signatures are not always present. In particular, the observation of an enhanced  $\alpha$ /proton density ratio is a good indicator of the presence of ejecta, as proposed by Hirshberg *et al.* [1972], but it is not observed in all ejecta, and it is not always a good measure of the extent of the ejecta. We shall discuss the relations between the fast ejecta and a “high  $\alpha$ /proton density ratio” of  $>8$ – $10\%$ . One finds that the  $\alpha$  particles do not provide a signature of the boundaries of the fast ejecta in most cases.

Bame *et al.* [1968] proposed that  $O^{6+}$  is the third most abundant ionic species in the solar wind, as expected from solar abundances and for a coronal temperature of  $1$ – $2 \times 10^6$  °K assuming thermal equilibrium [Hundhausen *et al.*, 1968; Hundhausen, 1968]. Occasionally, the density of  $O^7$  is greater than that of  $O^{6+}$ , implying a higher source temperature and suggesting that a  $O^{7+}/O^{6+}$  density ratio  $>1$  is a useful marker of material from a hot source. The  $O^{7+}/O^{6+}$  density ratio contains a coronal “fingerprint” of the solar wind source region and the expansion properties that is independent of interaction processes in the inner heliosphere and that is very complementary to in situ plasma observations [see, e.g., Buergi and Geiss, 1986]. During the expansion process from the coronal source, the ionic charge state adapts to the environment until the recombination and ionization timescales of a certain ionic charge state become large compared to the expansion timescale. At this point, the respective charge state freezes in. For a given speed, temperature, and density profile, each ionic charge state has its own specific freeze-in point, which may vary quite considerably from ion to ion. The  $O^{7+}/O^{6+}$  ratio typically

freezes in closer than one solar radius from the photosphere and therefore shows a lot of variability. It has been pointed out [see, e.g., *Geiss et al.*, 1995] that the charge state composition clearly distinguishes coronal hole-associated solar wind and streamer-associated slow solar wind. Furthermore, variations within low-speed solar wind also separate different sources of low-speed solar wind [*Zurbuchen et al.*, 2000; *Hefji et al.*, 2000]. An enhanced  $O^{7+}/O^{6+}$  density ratio is directly correlated only with magnetic clouds in the study of *Henke et al.* [1998]. The physical interpretation of this is not yet clear. Perhaps it relates to a higher source temperature, hotter plasma. In the case of magnetic clouds the magnetic field structure could make ion interaction with coronal electrons difficult, thus preventing them from achieving thermal equilibrium and resulting in a combination of both high and low charge states [*Ho et al.*, 2000; *Neukomm and Bochslter*, 1996]. Non-Maxwellian coronal distributions could also affect the freeze-in state [*Owocki and Scudder*, 1983]. The enhanced  $O^{7+}/O^{6+}$  could also be related to a difference in temperature history, due to the expected expansion effects of a plasma and a more rapid freeze-in process associated with that. This might be particularly expected for fast ejecta, where the expansion process around the freeze-in radius is clearly different from the ambient solar wind plasma. A density ratio  $O^{7+}/O^{6+} \approx 1$  corresponds to a coronal temperature of  $2 \times 10^6$  °K, and lower abundance ratios correspond to lower temperatures.

We consider regions in which the  $O^{7+}/O^{6+}$  density ratio is  $>1$  (because  $2 \times 10^6$  °K is at the high end of the coronal temperature range) and regions in which it is  $>0.7$  (in order to illustrate the sensitivity to the size of the region to the threshold chosen). In particular, we shall discuss the relations between the fast ejecta and the intervals when hour averages of  $O^{7+}/O^{6+} > 1$  and  $>0.7$  for  $\geq 4$  hours, using data from the Solar Wind Ion Composition Spectrometer (SWICS) [*Gloeckler et al.*, 1998] on ACE. We find a relation between high  $O^{7+}/O^{6+}$  density ratios and the front or rear boundaries of ejecta in some cases but not in others. Thus we cannot use this ratio to identify boundaries in general. More importantly, we show for the first time that complex ejecta as well as magnetic clouds have high  $O^{7+}/O^{6+}$  and variable density ratios.

*Montgomery et al.* [1974], *Bame et al.* [1981], and *Gosling et al.* [1987] identified bidirectional electron events with  $E > 80$  eV (also called counterstreaming electrons) and suggested that they are signatures of ejecta. *Gosling* [1990] proposed that counterstreaming electrons are synonymous with “CMEs” (ejecta). Strictly speaking, this is not true, as *Gosling* himself notes, since counterstreaming electron events can also be produced by interplanetary shocks and a connection to the Earth’s bow shock, for example. With experience and understanding of the plasma instrument, the counterstreaming electrons associated with shocks can often be identified and removed to produce a set of events that are probably associated with ejecta. We shall use such a set below, identified by members of the Los Alamos National Laboratory (LANL) group. However, there are ejecta (such as the magnetic clouds discussed by *Webb et al.* [2000a] and *Shodan et al.* [2000]) that are not accompanied by counterstreaming electrons. Thus one cannot identify all ejecta from electron data alone. Conversely, the observation of a counterstreaming electron event is not sufficient for identifying ejecta, as indicated by the observations of such electrons outside of but near magnetic clouds [e.g., *Skoug et al.*, 1999]. Finally, counterstreaming electrons might be present within ejecta, but they might also be present outside the ejecta, for

example, as a result of leakage from the ejecta or injection into a closed field region surrounding the ejecta. Despite all these caveats, when counterstreaming electrons (suitably chosen by an experienced observer and appropriately interpreted) are observed, they generally indicate the passage of ejecta.

Energetic bidirectional protons [*Palmer et al.*, 1978] and low-energy bidirectional protons [*Sanderson et al.*, 1983, 1985; *Marsden et al.*, 1987; *Richardson and Reames*, 1993; *Richardson et al.*, 2000] have also been interpreted as signatures for ejecta. However, bidirectional protons are not always present in ejecta, and many ejecta are not detected by this method [*Cane et al.*, 1999]. Moreover, when bidirectional protons are present, they do not always provide a good measure of the passage times of the ejecta.

Counterstreaming electrons happen to be present in all of the fast ejecta selected for study in this paper. The start time and end time of a counterstreaming electron event are sharply defined in general, but there may be brief intervals of unidirectional flows within the ejecta [see, e.g., *Larson et al.*, 1997]. We shall use the duration of a counterstreaming electron event between the start time and end time as one estimate of the passage time of ejecta (generally ignoring brief intervals of unidirectional electron streaming). This method can either overestimate or underestimate the extent of ejecta for the reasons given above. Nevertheless, the passage time of the ejecta is probably determined by the length of the interval of counterstreaming electrons within  $\sim 25\%$ , when counterstreaming electrons are present.

Since the events selected for this study were associated with fast flows, we can also estimate the passage time from the speed profile. The speed profiles have the form of a rapid increase in speed to a maximum value followed by a gradual decline in speed to some minimum value. Thus it is reasonable to associate the ejecta with the streams themselves, to some approximation. We shall take the “front boundary” as the time of maximum speed and the “rear boundary” as the time of minimum speed, since these times can be identified clearly in most cases. However, we recognize that the physical front boundary might occur a few hours ahead of the maximum speed (as it does for corotating streams) and that the rear boundary might occur a few hours after the minimum speed (since the rear end of the flow is often accelerated by a stream or shock advancing from behind). Thus the duration of the ejecta estimated from the maximum and minimum speeds might be a lower limit to the passage time of some of the ejecta we consider. Nevertheless, the time interval between the observation of maximum speed and minimum speed probably gives the passage time to within 25%.

In summary, one can identify possible boundaries of fast ejecta and estimate the passage times of ejecta in three ways: (1) by the magnetic cloud signature, for the magnetic clouds; (2) by the presence and duration of counterstreaming electrons, for ejecta in which such electrons are present; and (3) by the speed profile, for fast ejecta.

## 4. Discussion of Individual Events

### 4.1. List of Events

The fast ejecta that we selected are listed in Table 1. All of the four magnetic clouds and three of the complex ejecta were preceded by a shock. Each of the remaining two complex ejecta was preceded by an abrupt forward moving pressure wave (FPW). The first column of Table 1 identifies the ejecta as a

**Table 1.** Shocks and Ejecta Boundaries<sup>a</sup>

Type	Shock or FPW	Date	DOY	Magnetic Cloud (DOY)	Counterstreaming Electrons (DOY)	Stream (DOY)	Event
MC	shock	Feb. 18, 1999	49.090	49.6–50.5	49.5–51.4	49.6–50.6	1
MC	shock	May 1, 1998	121.891	122.5–123.9	122.2–124.0	122.4–123.7	2
MC	shock	Sept. 24, 1998	267.968	268.2–269.6	268.0–269.7	268.3–269.6	3
MC	shock	Nov. 8, 1998	312.181	312.8–314.1	312.4–314.1	312.3–313.8	4
CE	shock	May 3, 1998	123.708		124.3–127.9	124.3–127.2	5
	shock	May 4, 1998	124.094				
CE	FPW	July 5, 1998	186.136		187.9–191.2	187.2–191.2	6
CE	shock	Jan. 22, 1999	22.835		22.9–23.7	22.9–224.0	7
CE	FPW	July 30, 1999	211.430		211.6–215.4	211.9–215.5	8
CE	~shock	Sept. 22, 1999	265.490		265.8–269.5	265.8–269.3	9

<sup>a</sup>FPW, forward moving pressure wave; DOY, day of year; MC, magnetic cloud; CE, complex ejecta.

magnetic cloud (MC) or complex ejecta (CE). The second through fourth columns list the shocks and pressure waves; these columns give the date and the precise time in day of year (DOY) that the shocks and waves passed ACE. The fifth through seventh columns give the estimated start and end times at ACE for the magnetic clouds, the counterstreaming electron events, and the streams, respectively. Since some ejecta span one or more days and since the boundaries cannot always be determined unambiguously, we refer to the ejecta by an event number shown in the eighth column of Table 1 and/or by the date of the shock or pressure wave that precedes the ejecta.

#### 4.2. An Example of a Magnetic Cloud

A magnetic cloud (event 3) identified among the ejecta selected for this study, is shown in Figure 1. Its shock was observed on September 24, 1998. The format used in Figure 1 is the same as that used for all of the events discussed in this section. Figure 1a shows the magnetic field strength as a function of time measured by ACE. Figures 1b and 1c show the elevation angle  $\delta$  and the azimuthal angle  $\lambda$  of the magnetic field, in heliographic coordinates [Burlaga, 1995]. Figures 1d–1f show the density  $N$ , the proton temperature  $T$  (in units of  $10^5$  °K), and the solar wind speed  $V$ . The interval in which the  $\alpha$ /proton density ratio is high is shown by a horizontal bar in Figure 1d. The intervals in which the  $O^{7+}/O^{6+}$  density ratio is  $>1$  and  $>0.7$  for  $\geq 4$  hours are shown by the solid and dashed horizontal bars, respectively, in Figure 1f. Intervals in which counterstreaming electrons are present are shown by a horizontal bar in Figure 1e.

The magnetic cloud in Figure 1 is in the interval between the two vertical dotted lines where the magnetic field strength is high, the magnetic field direction rotates smoothly for more than a day, and the proton temperature is low. The magnetic cloud was associated with a fast stream, and the front boundary of the magnetic cloud corresponds to the time of maximum speed while the rear boundary corresponds to the time of minimum speed. Thus, in this case the boundaries of the ejecta determined by the criteria for identifying a magnetic cloud are essentially the same as those determined by the extreme of the speed profile.

Counterstreaming electrons were observed throughout the magnetic cloud, as shown by the horizontal bar in Figure 1e. However, the duration of counterstreaming electrons is larger than that of the magnetic cloud. The counterstreaming electrons are observed beginning a few hours after a shock shown by the solid vertical line,  $\sim 5$  hours before the front boundary

of the magnetic cloud shown by a vertical dotted line. In particular, the onset of the counterstreaming electrons appears in the interaction region, where the temperature is near its maximum value as a result of compression by the increasing speed. The counterstreaming electrons extend slightly beyond the rear boundary of the magnetic cloud shown by a vertical dotted line, during a period of a few hours in which the temperature is increasing and the speed is near its minimum values. Thus, in this case the duration of counterstreaming electrons is somewhat larger than that of the magnetic cloud and the declining speed interval in this event. In other events the counterstreaming electrons may underestimate the duration.

The magnetic field in Figure 1 was associated with intervals with an enhanced  $\alpha$ /proton density ratio, as illustrated by the horizontal bar in Figure 1d. The enhancement began near the front boundary of the magnetic cloud (or possibly earlier, when the high  $T$  makes measurements of  $\alpha$  particles difficult), it continued throughout the magnetic cloud, and it extended beyond the nominal rear boundary of the magnetic cloud. The uncertainties in the onset and termination times of the interval of the enhanced  $\alpha$  particle abundance are a few minutes in most cases. There are often large fluctuations in the  $\alpha$  particle abundance within an interval of enhancement, but we shall not discuss this feature.

In this event the intervals with  $O^{7+}/O^{6+} > 1$  and  $>0.7$ , shown by the solid and dashed horizontal bars, respectively, in Figure 1f nearly coincide with the region occupied by the magnetic cloud. However, this is not generally the case, as we shall show for some of the events in the remainder of section 4.

#### 4.3. An Example of Complex Ejecta

Complex ejecta (event 6) driving a forward pressure wave (FPW) observed on July 5, 1998, are shown in Figure 2. The boundaries of the ejecta determined from the maximum and minimum speeds in the stream are shown by the vertical dotted lines. Counterstreaming electrons and enhanced  $\alpha$  particle abundance were observed in the stream, ending when the speed reached its minimum value but beginning after the time of maximum speed. The passage time derived from the counterstreaming electrons is 12% smaller than that from the speed profile.

High temperatures were observed in the interaction region between the pressure wave and the maximum speed. It is likely that the front boundary of the stream, insofar as one exists, is in the interaction region, so that the ejecta might be larger than estimated from the interval in which the speed declines from

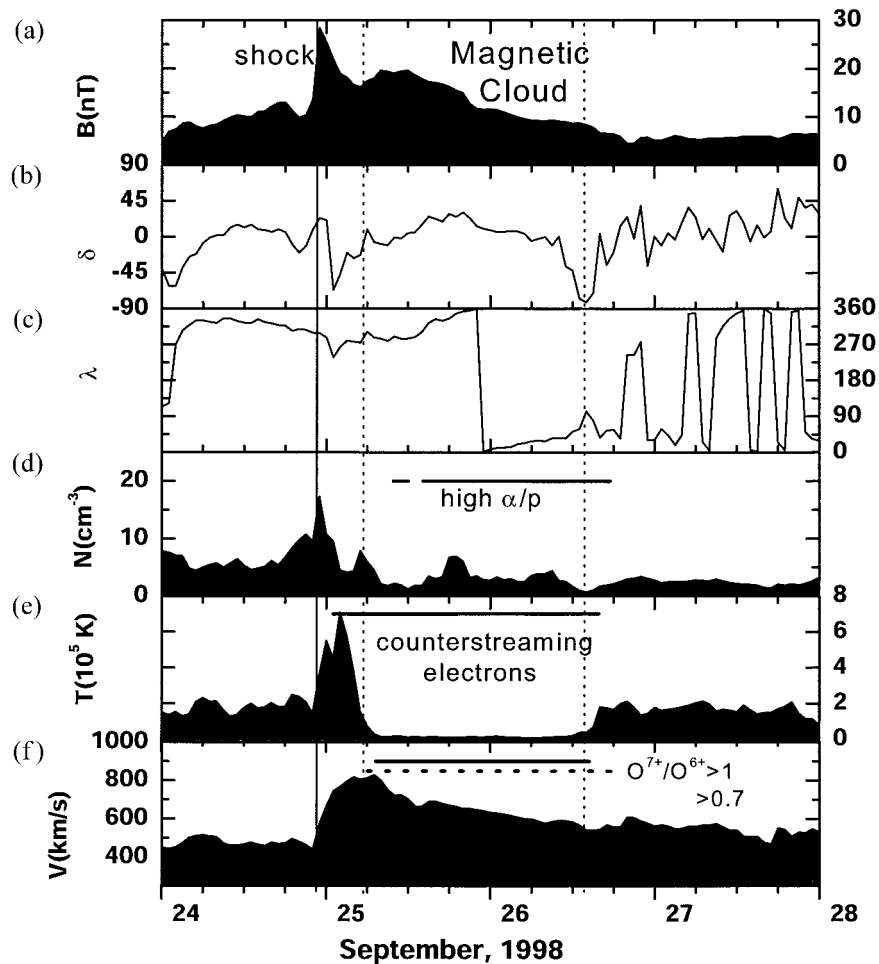


**Figure 1.** An example of a fast magnetic cloud, a magnetic cloud with a maximum speed greater than  $600 \text{ km s}^{-1}$ . (a) Magnetic field strength  $B$ , (b) magnetic field elevation angle  $\delta$ , (c) magnetic azimuthal angle  $\lambda$ , (d) proton density  $N$ , (e) proton temperature  $T$ , and (f) bulk speed  $V$ . Intervals in which the  $\alpha$ /proton density ratio is  $>8\text{--}10\%$  are shown by the horizontal bar in Figure 1d. The horizontal bar in Figure 1e shows the interval during which counterstreaming electrons were observed nearly continually. The solid and dashed horizontal bars in Figure 1f show the intervals during which  $\text{O}^{7+}/\text{O}^{6+} > 1$  and  $>0.7$ , respectively.

maximum to minimum values. Thus we again see the difficulties that are typically encountered in specifying the boundaries of the ejecta and the passage time of the ejecta. Nevertheless, one can reasonably assume that the passage time can be estimated with an accuracy of  $\sim 25\%$ . Most importantly, the passage time of the complex ejecta is long,  $\sim 4$  days.

The magnetic field direction in the ejecta shown in Figure 2 varies irregularly, which is a defining characteristic of complex ejecta. Although strong magnetic fields are often assumed to be a characteristic feature of ejecta, it is not the case for the ejecta in Figure 2. On the other hand, the proton temperature is low in this case, consistent with early ideas about the properties of ejecta.

Counterstreaming electrons are present throughout most of the ejecta as defined by the interval between the maximum and minimum speed. The  $\alpha$  particle abundance is also high throughout most of this lengthy interval. However, the  $\text{O}^{7+}/\text{O}^{6+}$  density ratio is not significantly greater than unity anywhere in this ejection. However, the  $\text{O}^{7+}/\text{O}^{6+}$  density ratio is  $>0.7$  in the middle of the complex ejecta, as shown by the horizontal dashed bar in Figure 2f.

#### 4.4. Other Magnetic Clouds and Ejecta

Here we present and discuss observations of the other magnetic clouds and complex ejecta listed in Table 1, in the same format as that in Figure 1. We comment briefly on a few of the characteristics of each event. By examining a number of events such as this, one can appreciate both the difficulties in identifying the boundaries of ejecta and the variety of possible structures. Nevertheless, it will be apparent that one can identify the presence of the ejecta and that the passage times of the ejecta determined in various ways can be estimated to within  $\sim 25\%$ .

Figure 3 shows a magnetic cloud (event 1) driving a shock observed on February 18, 1999. The duration of the magnetic cloud determined from the rotation of the magnetic field was  $\sim 1$  day. Enhanced  $\alpha$  particle abundance was observed within the magnetic cloud, but there was also an interval of enhanced  $\alpha$  particle abundance well behind the magnetic cloud. It is also possible that the  $\alpha$  particle abundance is high in the sheath, where  $T$  is so high that the  $\alpha$  particles are difficult to measure. Counterstreaming electrons were observed within the magnetic cloud, but weakly counterstreaming electrons were also

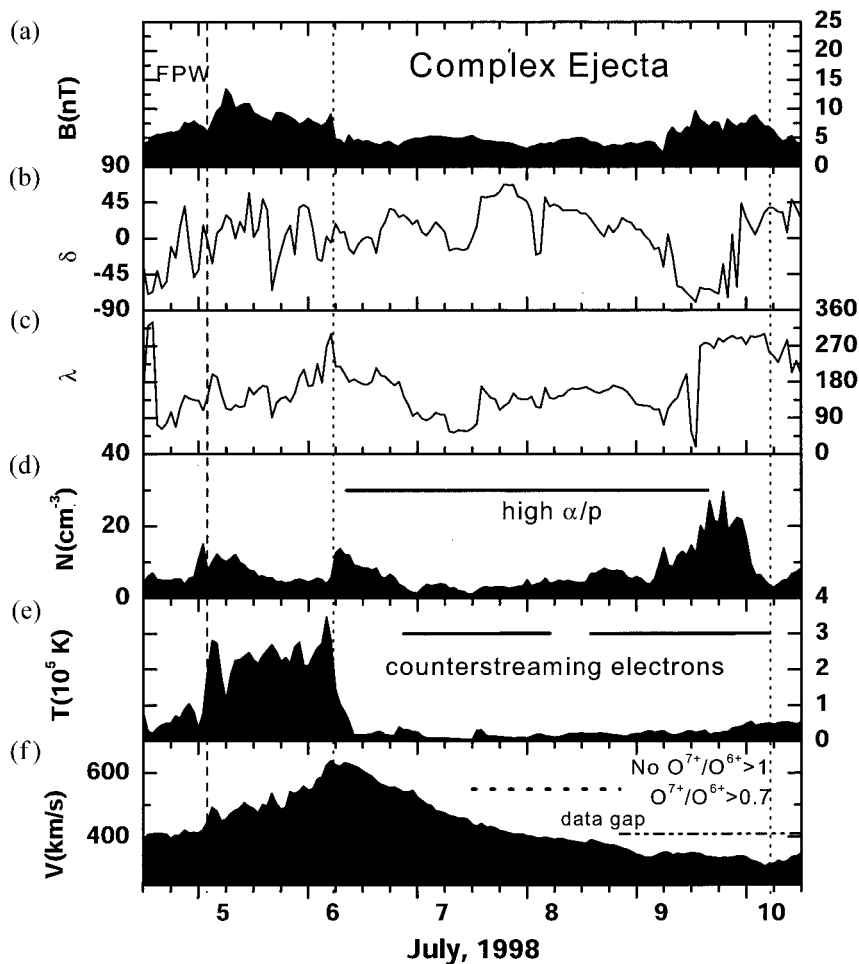


**Figure 2.** (a–f) An example of fast complex ejecta. The format is the same as that in Figure 1. FPW, forward pressure wave.

observed for  $\sim 18$  hours behind the magnetic cloud and intermittently for an additional 21 hours. The  $O^{7+}/O^{6+}$  density ratio was  $>1$  and  $>0.7$  in an interval that extended throughout the magnetic cloud but also throughout the sheath and even ahead of the shock. Thus the enhanced  $O^{7+}/O^{6+}$  abundance serves to identify the presence of the ejecta, but it does not define the boundaries in this case. The region of high  $O^{7+}/O^{6+}$  abundance also extends into the region behind the nominal magnetic cloud boundary, where counterstreaming electrons and an enhancement of the  $\alpha$  particle abundance were observed. This event has the notable feature that the magnetic cloud occupies only half of the ejecta defined by the interval between the maximum and minimum speeds and by the counterstreaming electrons and high  $\alpha$  particle abundance. One possible interpretation is that this event is a compound stream produced by two CMEs, one of which was associated with the magnetic cloud. Another possibility is that there is a wake or tail behind the magnetic cloud.

Figure 4 shows a magnetic cloud (event 4) driving a shock that was observed on November 8, 1998. The boundaries are not clearly defined, but the dotted lines show boundaries inferred from the magnetic field. The times of the maximum speed, counterstreaming electrons, and enhanced  $\alpha$  particle abundance are nearly the same, but they occur several hours ahead of the front boundary determined from the magnetic field data. The times of the passage of the rear boundary

determined by the magnetic field data, the counterstreaming electrons, the enhanced  $\alpha$  particle abundance, and  $O^{7+}/O^{6+} > 1$  are consistent within a few hours. However, the minimum speed occurs  $\sim 8$  hours earlier, perhaps because of an enhancement produced from a small stream behind the magnetic cloud. The region of  $O^{7+}/O^{6+} > 1$  is in the rear half of the magnetic cloud, whereas the region of enhanced  $\alpha$  particle abundance and counterstreaming electrons extends throughout the magnetic cloud and into the nominal sheath region behind the shock. The region of  $O^{7+}/O^{6+} > 0.7$  extends from before the shock to more than a day after the rear boundary of the magnetic cloud.

Figure 5 shows a magnetic cloud (event 2) on May 2, 1998, driving a shock that was observed on May 1, 1998. This event, notable for the extended presence of  $He^+$  and high  $\alpha$  to proton density ratio, was discussed in detail by Skoug *et al.* [1999]. The front boundary of the counterstreaming electrons occurs  $\sim 8$  hours earlier than that of the boundary defined by the magnetic field and near the time of the maximum speed, which is determined only to within  $\sim 6$  hours. The  $\alpha$  particle abundance was high throughout the magnetic cloud, beginning at the front boundary of the magnetic cloud. The  $O^{7+}/O^{6+}$  ratio was greater than one only near the front of the magnetic cloud; the interval with  $O^{7+}/O^{6+} > 0.7$  is somewhat longer, but it too begins at the front boundary of the magnetic cloud. The charge state composition of this magnetic cloud, described by Gloeck-

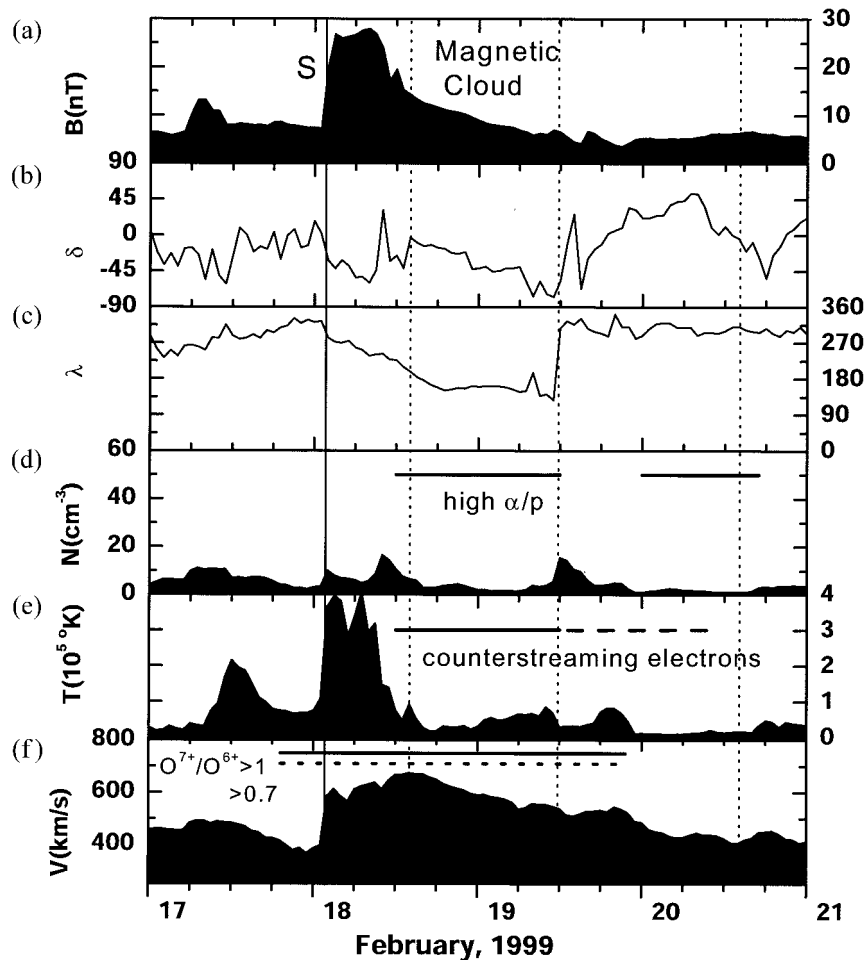


**Figure 3.** (a–f) A magnetic cloud followed by a flow, which could be either another ejecta or a wake. The format is the same as that in Figure 1.

ler et al. [1999], is highly unusual; it includes O charge states from  $O^{8+}$  to  $O^{2+}$ .

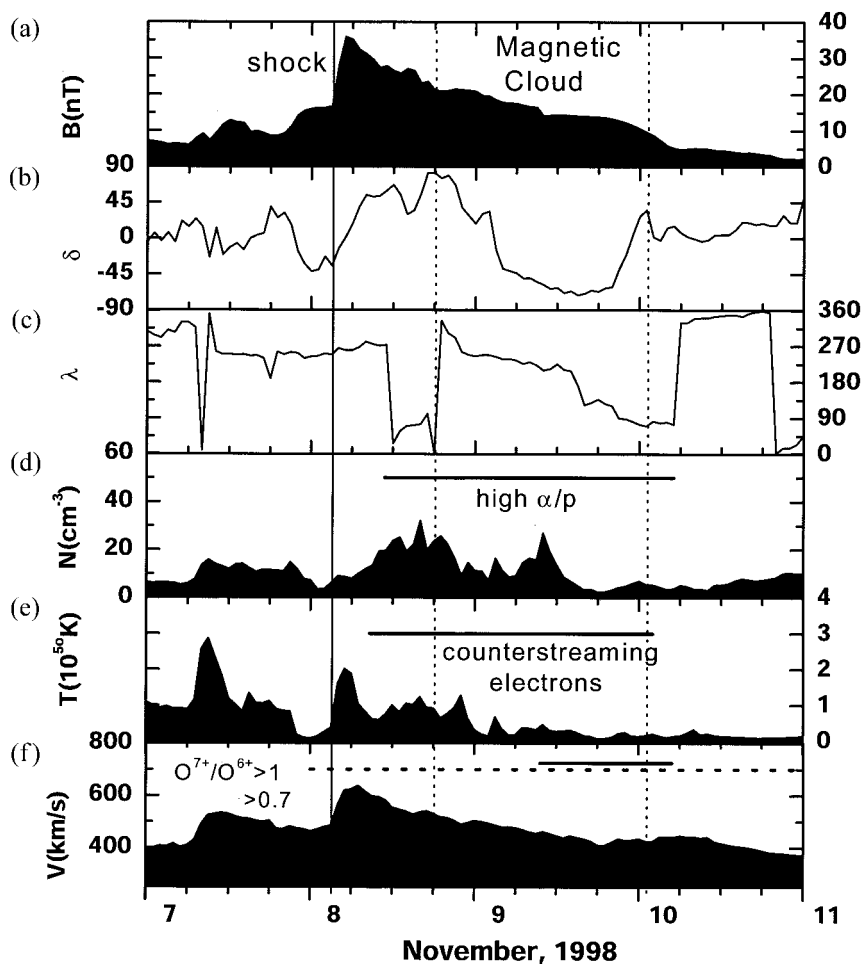
Figure 5 shows that the magnetic cloud was being overtaken by fast complex ejecta (event 5) driving a shock that was observed within the magnetic cloud on May 3, 1998. The times of the front boundary of the complex ejecta determined by the maximum speed and the counterstreaming electrons agree within a few hours. The minimum speed associated with the magnetic cloud occurs just ahead of the shock, so this is an example of an event whose size is underestimated somewhat by using the minimum speed to identify the rear boundary; however, one can see from Figure 5 that the error in the size of the magnetic cloud estimated in this way is certainly less than 25%. The time of the rear boundary determined from the minimum speed occurs  $\sim 15$  hours before that of the end of the counterstreaming electrons. The large fluctuations in  $T$  and  $V$  within the complex ejecta suggest that this event might have formed from a series of small mass ejections with various sizes, speeds, and temperatures. The  $\alpha$  particle abundance was high only in the rear of the complex ejecta. The  $O^{7+}/O^{6+}$  ratio was nowhere significantly greater than unity in the complex ejecta, but it was  $>0.7$  throughout the complex ejecta.

Figure 6 shows complex ejecta (event 7) driving a shock that was observed on January 22, 1999. The times of the front boundary determined from the counterstreaming electrons and from the maximum speed are nearly coincident. The time

of the rear boundary determined from the counterstreaming electrons occurs  $\sim 8$  hours before the minimum speed. In either case the passage time of the complex ejecta is comparable to that of the May 3, 1998, magnetic cloud (event 2) and much shorter than that of the other complex ejecta in this paper. The proton temperature in much of the ejecta is relatively high. The  $O^{7+}/O^{6+}$  density ratio was nowhere  $>0.7$ .

Figure 7 shows complex ejecta (event 8) driving a forward pressure wave observed on July 30, 1999. In this event a “compound stream” [Burlaga, 1975, 1984; Burlaga et al., 1987], with two speed maxima, was observed. Thus the complex ejecta might have been produced by the interaction of two CMEs. The first speed maximum occurs  $\sim 12$  hours after the pressure wave, which is a reasonable standoff time. The counterstreaming electrons arrive  $\sim 10$  hours before the speed maximum. The rear boundary of the electrons occurs several hours before the minimum speed, but the speed profile is very flat near the end of the stream, making a determination of the time of minimum speed relatively inaccurate. Enhanced  $\alpha$  particle abundance was observed sporadically within the complex ejecta, and it continued to be observed for more than a day behind the rear boundary. The  $O^{7+}/O^{6+}$  ratio was  $>1$  and  $>0.7$  in approximately the same interval near the rear of the complex ejecta.

Finally, Figure 8 shows complex ejecta (event 9) driving a shock observed on September 22, 1999. There appears to be a reverse wave tending to form a reverse shock in the leading



**Figure 4.** (a–f) A magnetic cloud in which the enhanced  $\alpha$  particle abundance and counterstreaming electrons extend ahead of the nominal front boundary of the magnetic cloud but extend throughout most of the fast stream. The format is the same as that in Figure 1.

part of the ejecta. The times of the front boundary determined from the peak speed, the counterstreaming electrons, and the enhanced  $\alpha$  particle abundance are in good agreement. They also coincide with a peak in the magnetic field strength. The rear boundary determined by the counterstreaming electrons occurs a few hours after that determined from the minimum speed, but a fast corotating stream following the ejecta was accelerating the rear of the complex ejecta, so that the minimum speed occurred before it would have in the absence of the corotating stream. The enhanced  $\alpha$  particle abundance occupied most of the complex ejecta, but it ended  $\sim 12$  hours earlier than the counterstreaming electrons. The  $O^{7+}/O^{6+}$  density ratio was  $>1$  for a relatively brief interval near the front of the complex ejecta, with no evident correlation to any other parameters. The  $O^{7+}/O^{6+}$  density ratio was  $>0.7$  in both the front and middle of the complex ejecta. The long passage time and the monotonic decrease in the speed suggest a localized source of relatively long duration, although the emission might have been intermittent.

We emphasize that all of the ejecta discussed above were associated with counterstreaming electrons. In the case of magnetic clouds this is generally believed to indicate that most magnetic field lines are connected to the Sun. Similarly, the counterstreaming electrons in complex ejecta suggest a magnetic topology with some sort of connectivity, despite the irregularity of the magnetic field directions.

## 5. Comparison of the Properties of Magnetic Clouds and Complex Ejecta

### 5.1. Magnetic Field Rotations

We have already noted that the magnetic field direction rotates smoothly during the passage of a magnetic cloud and irregularly during the passage of complex ejecta. This difference between the two types of ejecta is illustrated in Figures 9 and 10 for magnetic clouds and complex ejecta, respectively. Figures 9 and 10 show the elevation and azimuthal angles,  $\delta(t)$  and  $\lambda(t)$ , respectively, as a function of time in parametric form. For the magnetic clouds shown in Figure 9 the curve defined by  $\delta(t)$  and  $\lambda(t)$  is smooth for each magnetic cloud. Note that for the magnetic cloud (event 3) observed on September 25 and 26 (DOY 268 and 269), 1998, the rotation extends from  $\sim 270^\circ$  through  $360^\circ$  and farther to  $55^\circ$ . The shape and size of the arcs depend on the orientation of the magnetic clouds and the manner in which they are intercepted by ACE, but the essential point is that the variation is smooth in each case. This is in contrast to the variation of the magnetic field direction observed during the passage of complex ejecta, shown in Figure 10. For each of the complex ejecta the variation of the magnetic field direction is rather chaotic.

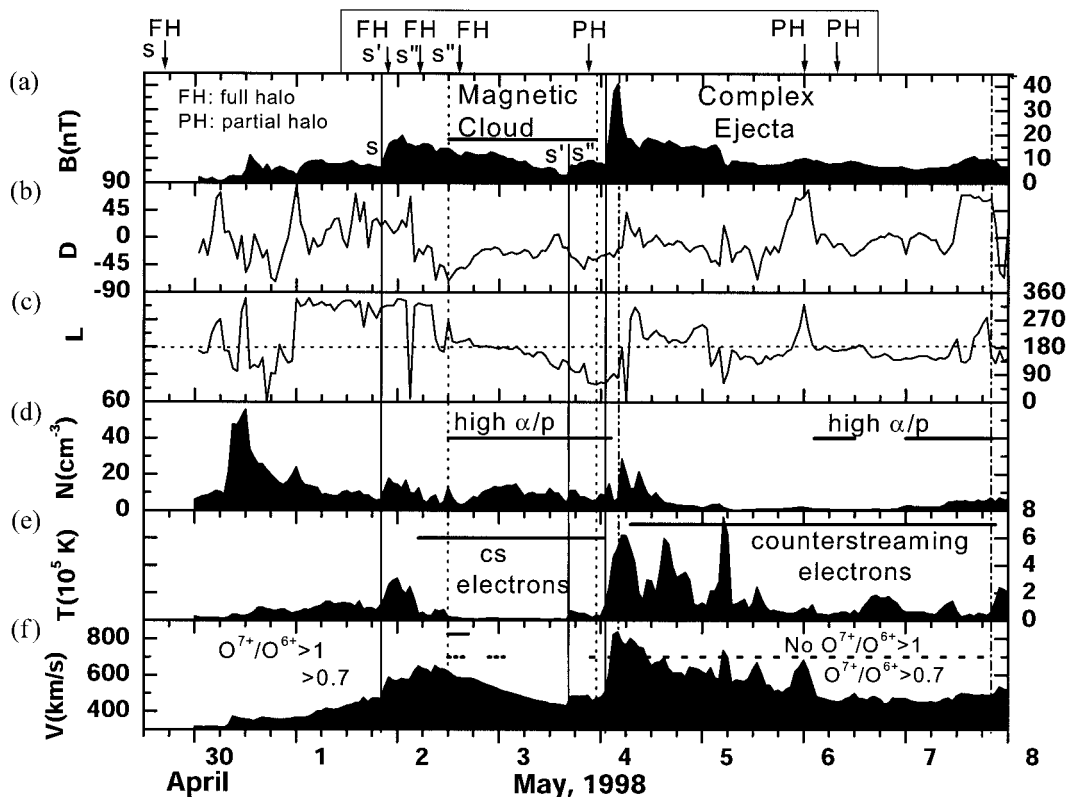


**Figure 5.** (a–f) A complex ejection (event 5) overtaking and interacting with a magnetic cloud (event 2). The format is the same as that in Figure 1. The magnetic cloud has the defining characteristics of a relatively high magnetic field strength, a smooth rotation in the magnetic field direction, and a low proton temperature. In addition, it has a declining speed profile indicating expansion, counterstreaming electrons indicating connection to the Sun,  $O^{7+}/O^{6+} > 1$ , enhanced  $\alpha$ /proton abundance, and  $He^+$  suggesting association with prominence material. The complex ejection has a long passage time (almost 4 days) as indicated by the counterstreaming electrons and the high  $\alpha$ /proton density ratio. The structure of the complex ejection is very complex, with highly variable magnetic field direction, both high and low proton temperatures, and both high and low magnetic field strengths. The simple magnetic cloud is related to a single solar source related to a full halo (FH) CME observed by Large-Angle Spectrometric Coronagraph (LASCO) on April 29, 1998, as shown by the arrow and “FH” in the top left corner of Figure 5. The complex ejection, on the other hand, was associated with at least three full halo CMEs and three partial halo (PH) CMEs, as indicated by the arrows and notation in the box at the top of Figure 5. Thus the long duration and complexity of the complex ejection could be the consequence of the interaction of several CMEs.

## 5.2. Average Plasma and Magnetic Field Parameters in the Ejecta

Given the boundaries of the ejecta, one can calculate the mean magnetic field strength  $B$ , proton temperature  $T$ , density  $N$ , speed  $V$ , and  $\beta$  in each of the ejecta and compare the means of these quantities for magnetic clouds and for complex ejecta. We used the maximum and minimum speeds to determine the front and rear boundaries, respectively, for calculating the averaging interval for each of the ejecta. The averages and the corresponding standard deviations of these quantities for the magnetic clouds and the complex ejecta are as follows. The average speed for the magnetic clouds ( $558 \pm 80 \text{ km s}^{-1}$ ) is comparable to that for the complex ejecta ( $500 \pm 63 \text{ km s}^{-1}$ ). The average magnetic field strength in the magnetic clouds is  $13 \pm 5 \text{ nT}$  compared to  $8 \pm 3 \text{ nT}$  for complex ejecta, and the average proton temperature in magnetic clouds is  $34,000 \pm 20,000 \text{ }^\circ\text{K}$  compared to  $100,000 \pm 80,000 \text{ }^\circ\text{K}$  for complex ejecta. It is significant that the magnetic field strengths and temperatures for complex ejecta are only slightly higher and lower, respectively, than the long-term average

values for the solar wind,  $6 \text{ nT}$  and  $150,000 \text{ }^\circ\text{K}$ , respectively. The average  $\beta$  for magnetic clouds is  $0.06 \pm 0.04$ , whereas that for complex ejecta is  $0.25 \pm 0.09$ . The relatively high  $\beta$  in the complex ejecta are consistent with the irregular variations in the magnetic field direction. A possible relation between the high  $\beta$  and turbulence is obvious. Mechanisms for the origin of the complex ejecta with high  $\beta$ , such as a pressure-driven instability [Wysocinski *et al.*, 1988], remain to be investigated.

## 5.3. Passage Times of the Ejecta

We can estimate the passage times of ejecta by the duration of counterstreaming electrons and by the speed profile. For magnetic clouds one can also estimate the passage time from the magnetic cloud boundaries determined in the traditional way based on the field and temperature profiles.

For the magnetic clouds the average passage time is  $1.20 \pm 0.19$  days based on the magnetic cloud signature and  $1.27 \pm 0.21$  days based on the stream profile, so these two estimates are essentially the same. The average passage time based on

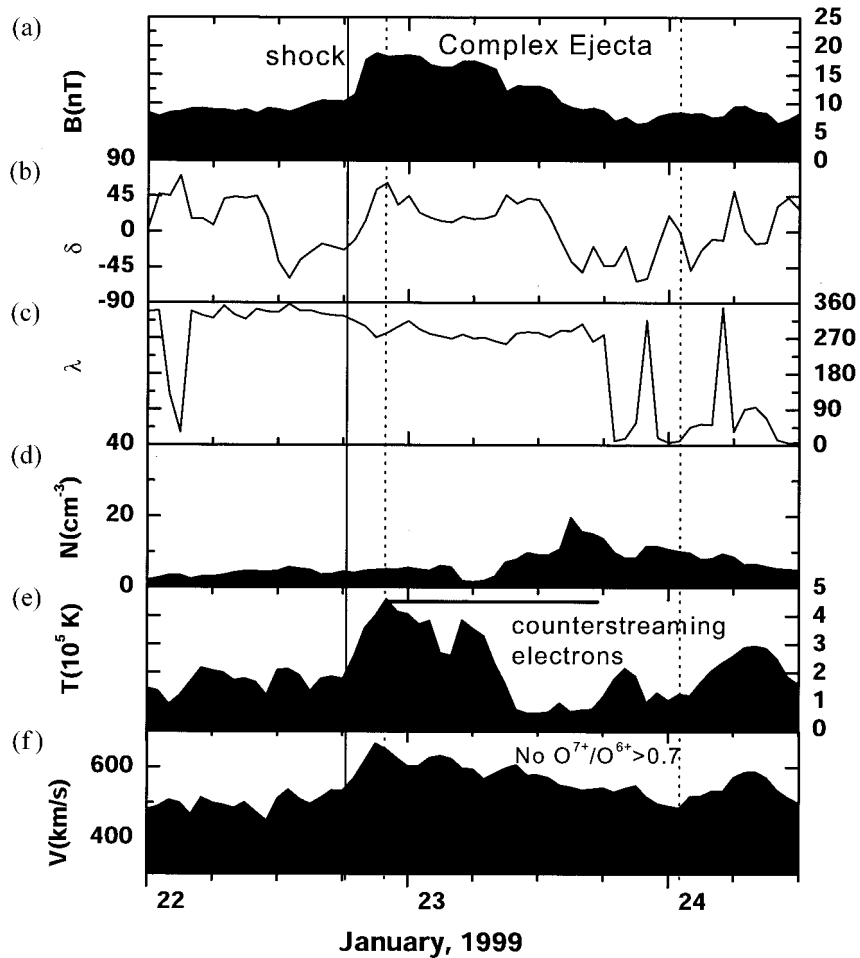


**Figure 6.** (a–f) Fast complex ejecta with a relatively small passage time. The format is the same as that in Figure 1.

the counterstreaming electrons is  $\sim 15\%$  larger, namely,  $1.55 \pm 0.37$  days.

For the complex ejecta the average passage time is  $3.1 \pm 1.1$  days based on the stream profiles and  $3.1 \pm 1.3$  days based on the counterstreaming electrons. Thus the average passage time determined by these two methods is essentially the same, even though the start and end times differ in some instances.

The passage times (“durations”) for the individual magnetic clouds and complex ejecta, determined by the three different methods discussed above, are illustrated in Figures 11a and 11b, respectively. For all of the magnetic clouds the passage time derived from the magnetic cloud signatures is essentially the same as that derived from the stream profiles. The passage time derived from the counterstreaming electrons is  $\sim 25\%$  larger than that derived from the magnetic cloud signature for three of the magnetic clouds, and it was the same as that derived from the magnetic cloud signature for the fourth magnetic cloud. For the complex ejecta the passage time derived from the counterstreaming electrons was larger than that derived from the speed profile in two of the cases, smaller in two cases, and essentially the same in one case. Thus there is no systematic difference between the passage times derived from the counterstreaming electrons and those from the speed profiles for complex ejecta.

The most significant result from the observations discussed above is that the passage times for all of the complex ejecta

except one are  $\sim 3$  times greater than those for magnetic clouds. Only one of the complex ejecta (event 7) had a passage time comparable to that for magnetic clouds. The average passage time for all of the complex ejecta is  $\sim 2.3$  times greater than that for magnetic clouds. It is possible that the large passage time of the complex ejecta in our sample is related to the ascending phase of the solar cycle, since smaller passage times were reported in earlier studies [e.g., Gosling, 1990]. The existence of large passage times for most complex ejecta is significant and requires an explanation. Since the passage time of the complex ejecta can be comparable to the transit time to 1 AU, one cannot attribute its large magnitude to the expansion of some small structure ejected from the Sun, as one does for magnetic clouds. It is more likely that the total emission time interval of a complex ejection is of the order of a few days.

#### 5.4. Length Scales of the Ejecta

One can calculate a length scale for each of the ejecta by taking the ratio of the mean speed to the passage time of ejecta. The length scale would represent a radial cross section if the ejecta have the form of an annulus, but more likely it represents a convolution of radial, azimuthal, and temporal effects.

For the magnetic clouds the average length scale from the speed profiles ( $0.41 \pm 0.06$  AU) is essentially the same as that from the magnetic cloud signatures ( $0.39 \pm 0.08$  AU). The

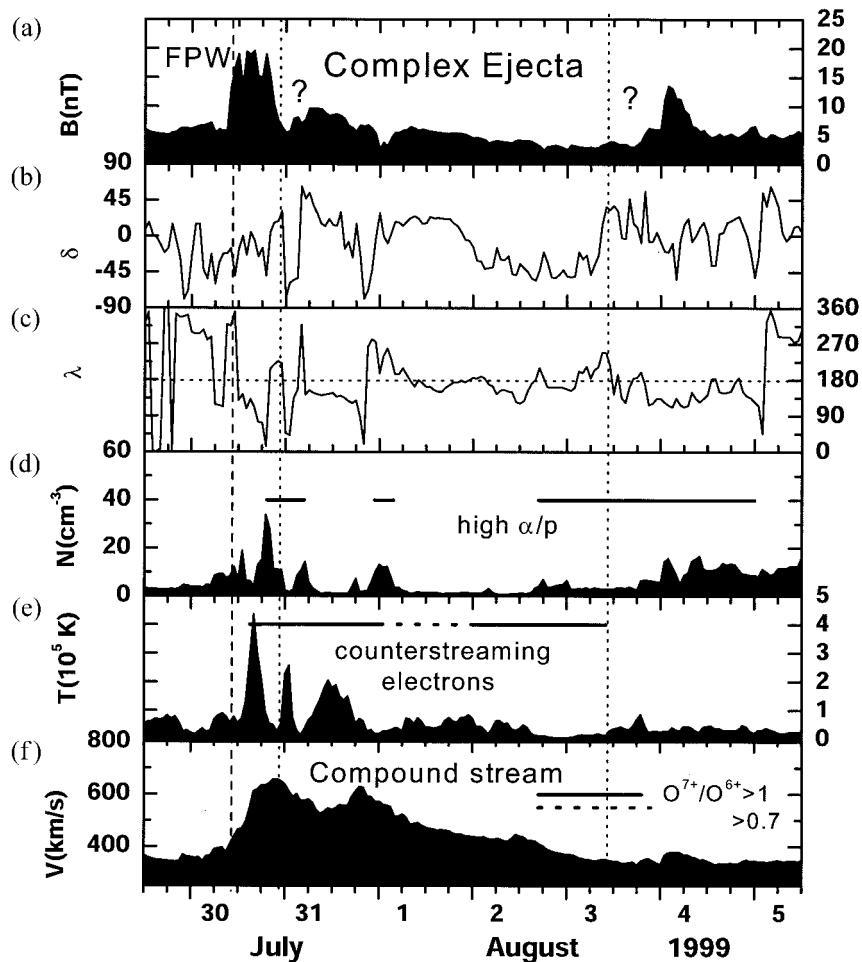


**Figure 7.** (a–f) Fast complex ejecta associated with a compound stream, possibly produced by two CMEs.

average length scale derived from the counterstreaming electrons ( $0.50 \pm 0.12$  AU) is 25% larger than that derived from the other methods. All of these length scales are larger than the typical radial cross section of the magnetic clouds discussed in the literature, which is  $\sim 0.25$  AU [Klein and Burlaga, 1982; Lepping *et al.*, 1990].

For the complex ejecta the average length scale computed from the counterstreaming electrons ( $0.85 \pm 0.35$  AU) is the same as that computed from the speed profile ( $0.85 \pm 0.26$  AU). Since the length scale is comparable to 1 AU, one cannot regard this scale as simply a radial cross section of the ejecta; one is sampling different longitudinal portions of the ejecta as it moves past the spacecraft. Nevertheless, it is clear that some fast complex ejecta can have relatively large radial length scales of the order of 1 AU.

The length scales for the individual magnetic clouds and complex ejecta are shown in Figures 11c and 11d, respectively. The length scale of magnetic clouds derived from counterstreaming electrons is greater than that derived from the speed profile and from magnetic cloud parameters in three of the four cases. One of the complex ejecta (event 7) has a length scale comparable to that of the magnetic clouds, but the others are  $\sim 3$  times as large as the magnetic clouds.

The important conclusion from the above results is that the length scale of complex ejecta is typically 3 times that of the magnetic clouds. This ratio is comparable to that for the passage times, since the mean speed of the magnetic clouds is

nearly the same as that for the complex ejecta. Possible explanations of this result are discussed in section 9.

## 6. Solar Origins of the Ejecta

### 6.1. General Results

We have examined the possible solar origins of each of the nine fast ejecta listed in Table 1 and discussed above. Our results are summarized in Table 2. Four caveats must be considered in the interpretation of the results in Table 2. First, the events occurred in the period from February 1998 to September 1999, during the rise to solar maximum of this cycle. Thus the magnetic complexity of the Sun and the level of activity increased during this period, making it difficult to identify the source regions unambiguously. Second, for four of the ejecta (events 1, 3, 6, and 7) there were no Solar and Heliospheric Observatory (SOHO) data and thus no confirmation of the launch of halo-type CMEs. Third, it is difficult to identify the sources of the ejecta at 1 AU because the travel time from the Sun to 1 AU is often greater than the time between events on the Sun. However, we do have the SOHO LASCO and extreme ultraviolet imaging telescope (EIT) observations of halo CMEs for some events. Moreover, since we selected ejecta with speeds  $> 600$  km s $^{-1}$  the travel times are  $< 70$  hours; we used this travel time as an upper limit to determine possible solar sources. Fourth, it is usually difficult to completely rule out the association of one source from another when they

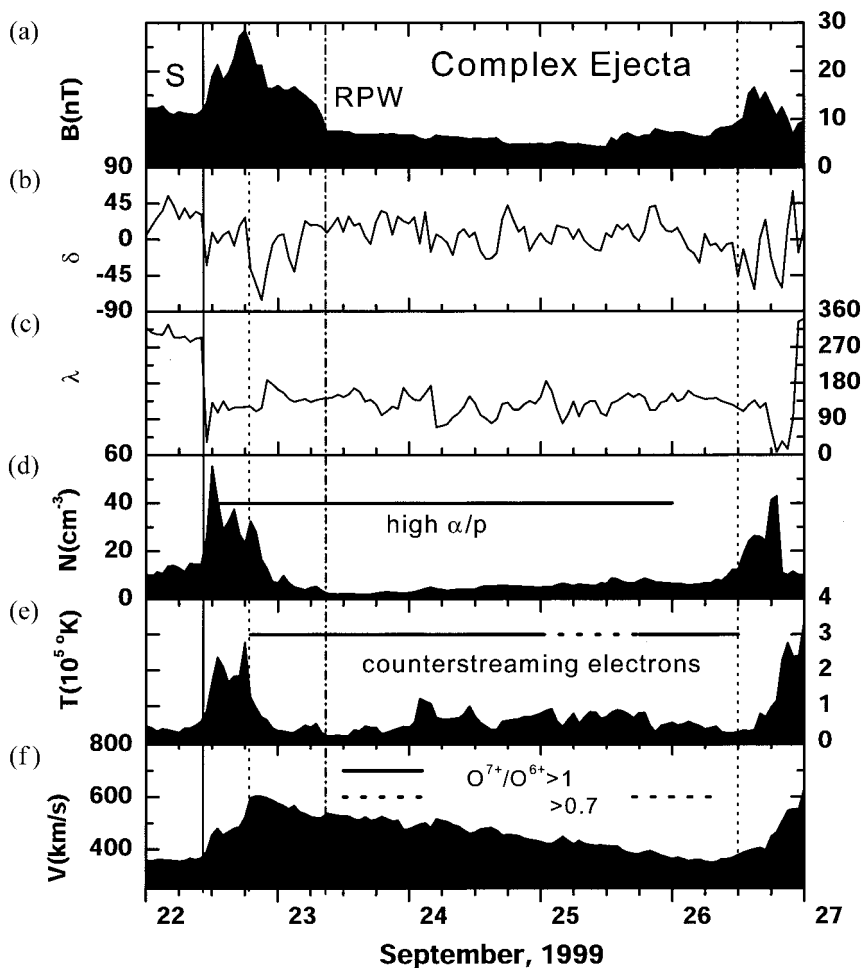


**Figure 8.** (a–f) Complex ejecta with a passage time of  $\sim 4$  days. Such an event could be produced by a lengthy emission of a single CME or a series of small ejecta. The format is the same as that in Figure 1. RPW, reverse pressure wave.

occur within a fairly broad occurrence window such as ours, so that some of our results are ambiguous.

Despite these limitations, we can draw the important conclusion that most of the magnetic clouds probably had a single source, whereas nearly all of the complex ejecta could have had multiple sources.

Three of the four magnetic clouds (the exception is event 1) were consistent with arising from a single solar source. Each of these three magnetic clouds was associated with at least four of the following: (1) a halo CME, (2) a big, long-duration flare (X-ray flare  $> M5$ ; optical importance 2 or 3; duration  $> 2$  hours), (3) a disappearing filament (DSF), (4) coronal dimming regions, and (5) coronal waves, all within  $25^\circ$  of geometrical Sun center. (There were no SOHO data for the magnetic cloud of event 3, so one of these halos is inferred.) These results support those found by *Webb et al.* [2000a, 2000b, 2000c] and *St. Cyr et al.* [2000].

Four of the five complex ejecta could have had multiple sources. There were 10 of these multiple candidate sources. Significantly, one complex ejection (event 9) probably had a single source; there was a full halo CME, a pure disappearing filament with no major flare, and a coronal dimming region. However, unlike the magnetic clouds, the halo was faint, and the filament eruption/X-ray arcade was south of Sun center. There were no SOHO data for two of the complex ejecta,

events 6 and 7, making it more difficult to distinguish among multiple candidate sources. For each of the complex ejecta, the two to four candidate sources were judged to have roughly an equal probability of being associated with the complex ejection, based on disk location, the type and degree of activity, and the travel time to 1 AU. In general, the possible sources of complex ejecta had these characteristics: (1) partial or full halo CMEs, (2) moderate flares (X-ray flare  $< M2$ ; optical importance, 1 or subflare), and (3) flare durations shorter than those associated with the magnetic clouds. About half of the complex ejecta had clear DSF, dimming, and wave signatures. With one exception (event 9; see below) the candidate source locations were as close to Sun center as the magnetic cloud sources were.

## 6.2. Example of Sources for a Magnetic Cloud and a Complex Ejection

The different nature of the sources of magnetic clouds and complex ejecta is illustrated clearly by the magnetic cloud (event 2) and complex ejecta (event 5) shown in Figure 5, which were observed by ACE in front of the Earth. The vertical arrows at the top of Figure 5 show the onset times of all large LASCO CMEs occurring from 3 days before the May 1, 1998, shock through the 1-week interval in Figure 5. The following abbreviations are used in Figure 5 to describe the types of CMEs: FH, Full halo CME; and PH, partial halo CME. All of

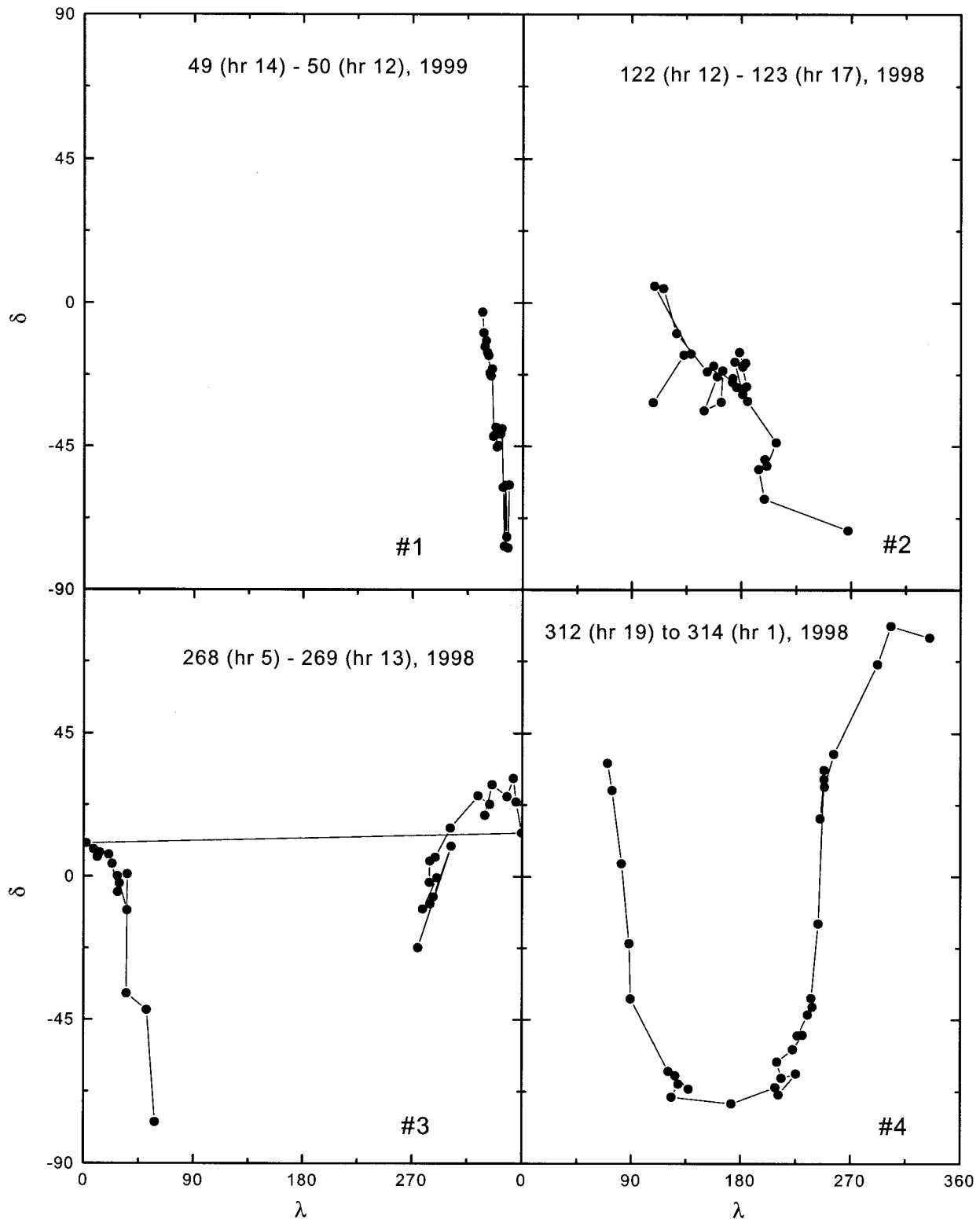


**Figure 9.** Plots of  $\delta$  versus  $\lambda$  for each of the four fast magnetic clouds. The observations trace out a smooth curve as the magnetic clouds move past ACE, consistent with ordered magnetic flux rope structures.

the halo events were associated with activity from just one active region, region 8375, which produced an unusual series of similar, energetic events during its disk passage [Wang *et al.*, 2000; Thompson *et al.*, 2000].

The magnetic cloud (event 2) and the first shock observed by ACE on May 1–3 (Figure 5) are associated with the single,

relatively isolated, energetic full halo CME observed by LASCO on April 29, 1998, as indicated by the arrow and notation on the top left of Figure 5. The travel time is 52 hours, in good agreement with the wind speed behind the shock of  $\sim 640 \text{ km s}^{-1}$ .

The complex ejecta (event 5) in Figure 5 could have been

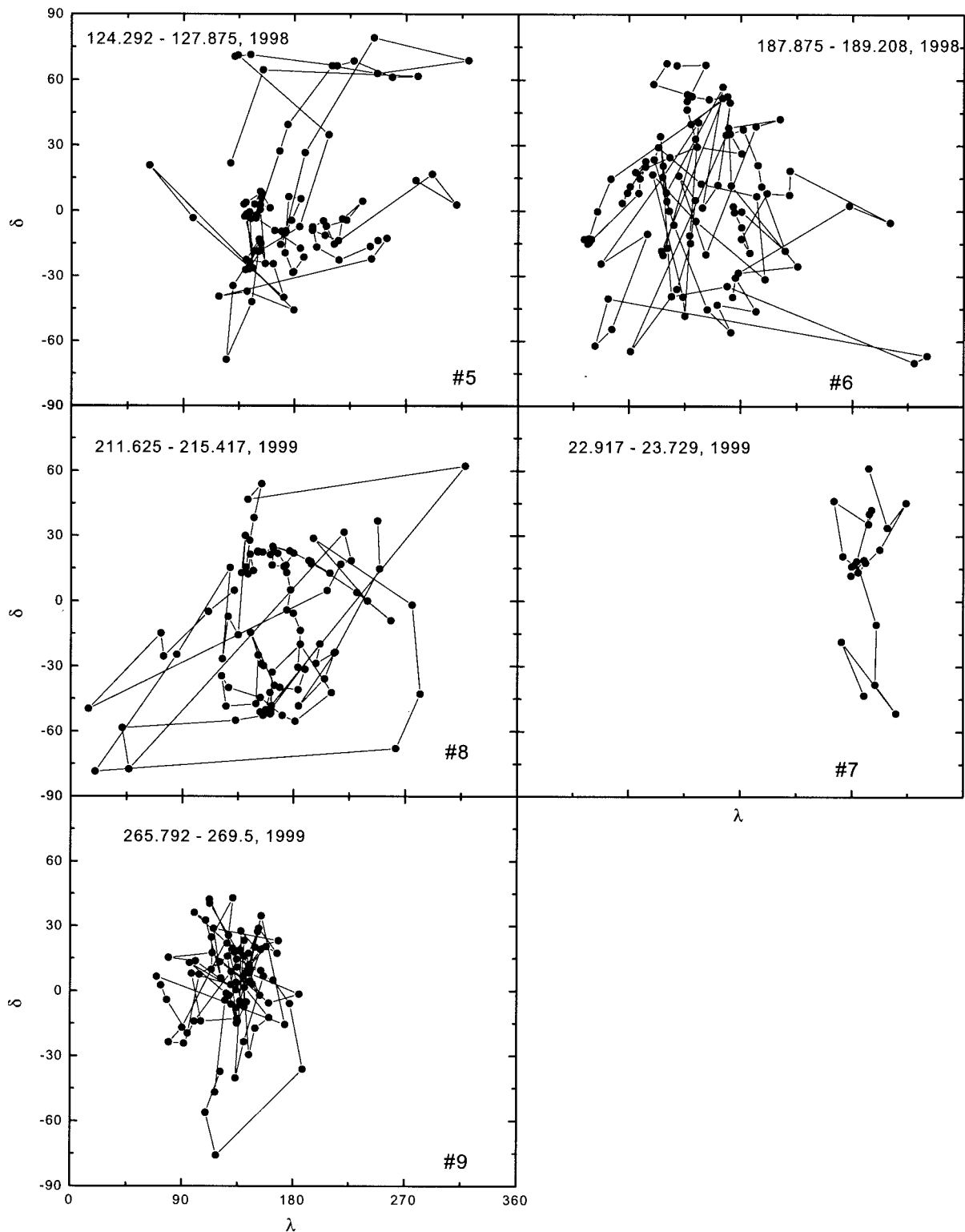


**Figure 10.** Plots of  $\delta$  versus  $\lambda$  for each of the five fast complex ejecta. The observations trace out a chaotic pattern as the complex ejecta move past ACE, indicating the lack of ordered magnetic field structures.

caused by the interaction of the three full halo CMEs and the later three partial CMEs indicated by the arrows and notation in the box at the top of Figure 5. The interaction and intermingling of some or all of these FH and PH CMEs would explain the complex form and relatively long duration of the complex ejecta. Note that all the plasma and magnetic param-

eters of the complex ejecta were highest during May 4 and early May 5, within 1.5–4 days of the onsets of the three full halo CMEs. The shocks were observed by ACE on May 3, 1998, and could be related to the three full halo CMEs observed by LASCO on May 1 and 2, 1998, indicated in the box at the top of Figure 5. In particular, it is possible that the

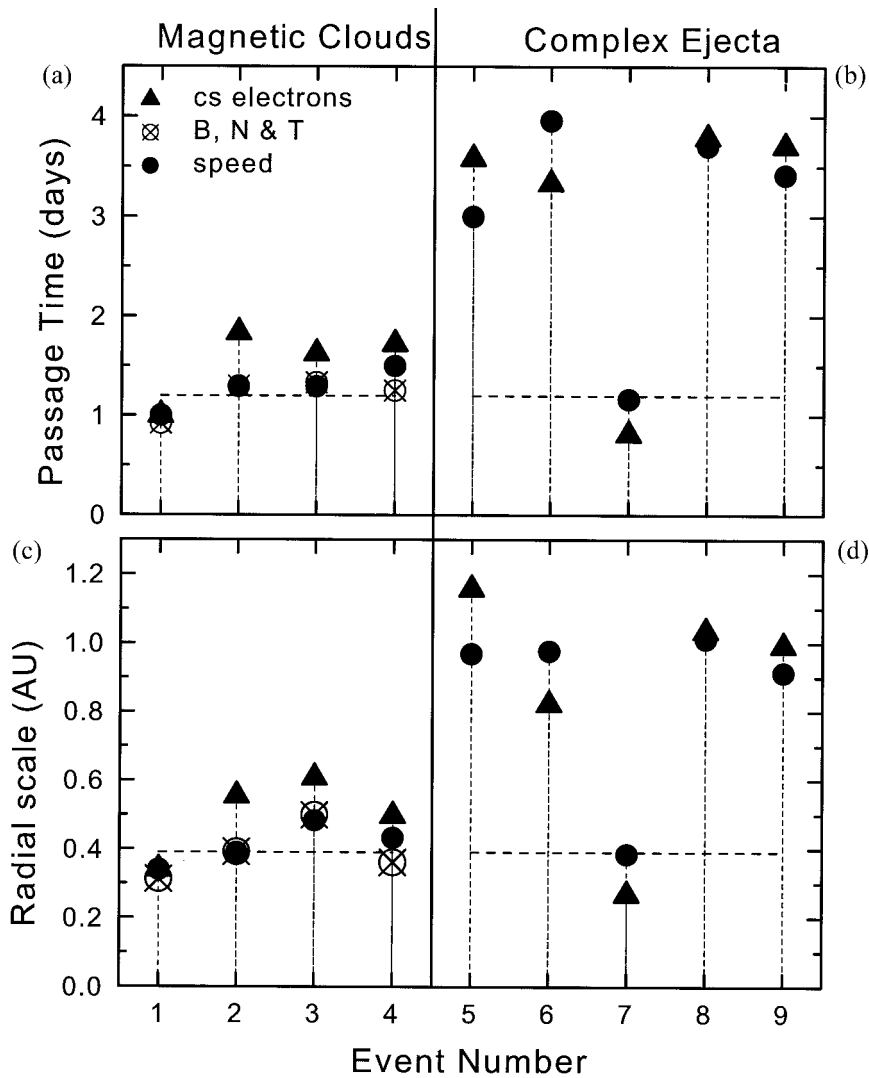


**Figure 11.** (a, b) The passage times (durations) for each of the fast ejecta and (c, d) the characteristic scales (passage time divided by mean speed) for each of the fast ejecta.

**Table 2.** Candidate Solar Sources of Ejecta<sup>a</sup>

Onset Date	Time, UT	Association With Ejecta?	Halo CME	Flare Size	Duration, hours	Distance, deg	DSF?	Dimming?	Wave?	Event/Type
Feb. 15, 1999	2140	maybe	...	small	1.5	16	yes	no	...	1/MC
Feb. 16, 1999	0315	maybe	...	moderate	2.5	18	?	no	...	
April 29, 1998	1615	yes	FH	big	>12	25	yes	yes	yes	2/MC
Sept. 23, 1998	0640	yes	...	big	>4	14	yes?	?	...	3/MC
Nov. 5, 1998	1830	yes	FH	big	>5	25	?	yes	yes	4/MC
May 1, 1998	2225	maybe	FH	moderate	~1	45; 15	no	yes	yes	5/CE
May 2, 1998	0435	maybe	FH	moderate	1.5	19	no?	yes	yes	
May 2, 1998	1044	maybe	FH	big	4.5	14	no?	yes	yes	
May 3, 1998	2120	maybe	PH	moderate	1.5	35; 32	yes	yes	yes	
July 3, 1999	0107	maybe	...	moderate	3	33	?	?	...	6/CE
Jan. 19, 1999	1500	maybe	...	no?	...	36	yes	no	...	7/CE
Jan. 20, 1999	>1500	maybe	...	no?	...	25	no?	no?	...	
Jan. 20, 1999	1900	maybe	...	big	>8	~80	yes	yes?	...	
July 28, 1999	0152	maybe	FH	moderate	1.5	22	?	no?	no?	8/CE
July 28, 1999	0805	maybe	FH	moderate	<1	21	?	no?	no?	
Sept. 20, 1999	0500	yes	FH	small	~1.5	38	yes	yes	no	9/CE

<sup>a</sup>CME, coronal mass ejection; DSF, disappearing filament; FH, full halo; PH, partial halo.

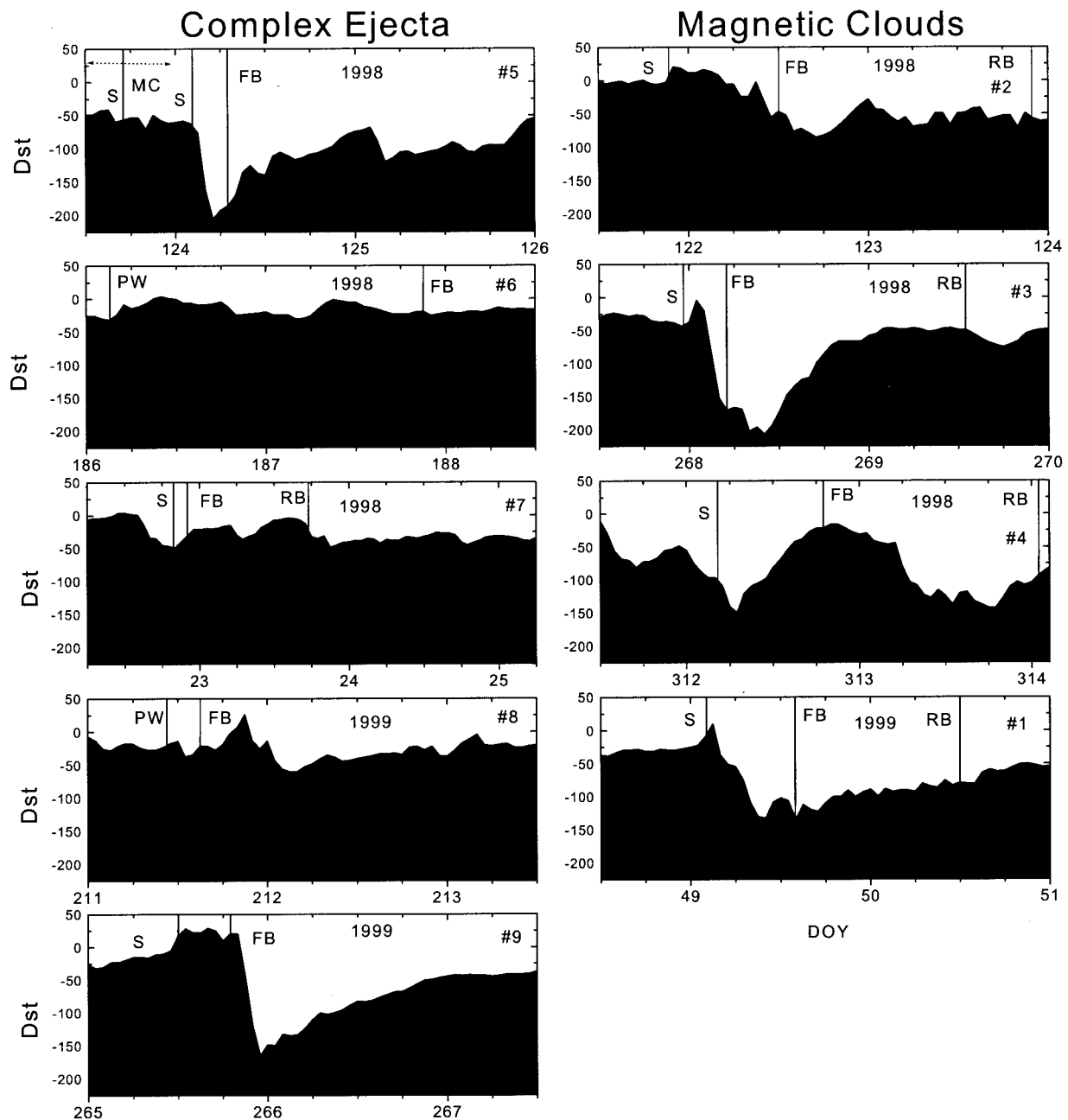


**Figure 12.** *Dst* variations associated with the magnetic clouds and complex ejecta. All of the magnetic clouds produced large geomagnetic storms, but most of the complex ejecta did not. S, shock; PW, pressure wave; MC, magnetic cloud; FB, front boundary; RB, rear boundary.

shocks associated with the second and third full halo CMEs could have merged to produce the shock observed at ACE on May 4, 1998.

## 7. Geomagnetic Effects of Ejecta

Since ejecta were initially postulated to explain the cause of geomagnetic storms, it is not surprising that there is a large literature concerning their relation between in situ observations of ejecta and geomagnetic storms [see, e.g., Akasofu and Chapman, 1972; Tsurutani *et al.*, 1988; Gosling *et al.*, 1990; Webb *et al.*, 1993, 2000b]. Dungey [1961] and Baker *et al.* [1984] showed that a fast solar wind speed and a strong southward component of the magnetic field are particularly effective in

producing geomagnetic activity. The *Dst* index is one useful measure of the geoeffectiveness of ejecta. Figure 12 shows the *Dst* index during a 2.5-day interval for each of the events discussed above. The location of the leading shock (S) or pressure wave (PW) is shown by a vertical line. The estimated front and rear boundaries (FB and RB) are also shown by vertical lines. The passage time of four of the complex ejecta is so long that the rear boundaries are off scale. No allowance is made for the propagation time from ACE to Earth, so that a *Dst* disturbance follows a shock pressure wave, or ejecta boundary by approximately an hour.

Each of the magnetic clouds was preceded by a shock, which compressed the magnetosphere and produced an increase in *Dst*. Each of the magnetic clouds also produces a significant

geomagnetic disturbance indicated by a decrease in  $Dst$ . The geoeffectiveness of magnetic clouds is well known [Burlaga *et al.*, 1981, 1987; Zhang and Burlaga, 1988; Webb *et al.*, 2000b]. The peak  $Dst$  values for the magnetic clouds in Figure 12 are  $-85$ ,  $-207$ ,  $-149$ , and  $-132$ , from top to bottom, respectively. A part of each magnetic cloud contains strong southward magnetic fields that caused a decrease in  $Dst$  at various times relative to the shock, depending on the structure and speed of the magnetic cloud. The sheath between the shock and the front boundary of the magnetic cloud may also contain compressed southward magnetic fields that contribute to the geomagnetic activity in varying degrees. The sheath contribution is substantial in two of the events. The effectiveness of a southward component of the magnetic field is greater when the speed is higher.

The fast complex ejecta are less geoeffective than the magnetic clouds in general, despite their larger passage times, as shown in the panels on the left side of Figure 12. Three of the complex ejecta shown in Figure 12 produced no major geomagnetic activity; however, one must consider that these events occurred during the solstice periods when ejecta tend to be less geoeffective [Crooker and Cliver, 1994]. One complex ejection (event 5), shown in the top left panel, produced  $Dst$  as low as  $-205$ , but it did so indirectly by driving a shock and pressure wave into the rear of a magnetic cloud with strong southward fields (see Figure 5). The complex ejecta (event 9) shown in the lower left panel of Figure 12 also produced a large geomagnetic storm, with a minimum  $Dst = -164$ . In this case the geomagnetic storm was associated with strong southward magnetic fields at the front of the ejecta and in the interaction region driven by the complex ejecta (see Figure 8). Since some complex ejecta are themselves not geoeffective, the detection of a CME moving toward Earth (e.g., by the observation of a halo event) might lead to a false prediction of a magnetic storm if the CME is related to complex ejecta. Nevertheless, two of the complex ejecta we examined did produce magnetic storms, principally by their interactions with material ahead of the ejecta.

All six of the ejecta that were associated with large geomagnetic storms (peak  $Dst < -85$  nT) were also associated with one or more full halo CMEs with front-side solar activity. The probability of the association is greater for events 2, 3, 4, and 9 than for events 5 and 1). Five of these six geomagnetic storms were intense, i.e., peak  $Dst < -100$  nT. These results are consistent with the results of Webb *et al.* [2000b]. Four of the six geomagnetic storms were associated with both flares and disappearing filaments. The complex ejection of event 9 was a DSF/arcade-only event.

## 8. Summary of the Observations

We identified the fast ejecta at 1 AU (transient, noncorotating flows that move past the Earth during a day or more, with a maximum speed  $>600$  km  $s^{-1}$ ) in the interval from February 5, 1998, to November 29, 1999, during the ascending phase of solar cycle 23, using ACE magnetic field and plasma data. Two classes of ejecta were defined, magnetic clouds and complex ejecta. The magnetic clouds have ordered magnetic field directions by definition, but the complex ejecta have disordered magnetic field directions. The rate of occurrence of the fast ejecta in the 1.8-year interval is 5 per year or 0.4 per month. Nearly half of the ejecta (4/9) are magnetic clouds in

the small set of events that we examined during the period of increasing solar activity.

Three methods were used to estimate the boundaries of the fast ejecta: one based on the signature of magnetic clouds (for the magnetic clouds only), a second based on counterstreaming electrons, and a third based on the speed profile. Although the three methods do not always give the same boundary positions, the passage times determined by the three methods agree within 25%. The average passage time of the complex ejecta (3 days) is  $\sim 2.3$  times that for the magnetic clouds. Using the measured speeds, a length scale was computed for each of the ejecta. The mean speed of the magnetic clouds ( $558 \pm 80$  km  $s^{-1}$ ) is comparable to that for the complex ejecta ( $500 \pm 63$  km  $s^{-1}$ ). The average length scale of the complex ejecta (0.85 AU) was 1.9 times that of the magnetic clouds. Although the numbers have significant uncertainties, it is clear that some of the complex ejecta have large passage times and scale lengths compared to the magnetic clouds. This fact is surprising, and it is not understood. We discuss some possible explanations in the following section.

A magnetic cloud, by definition, has higher than average magnetic field strength, low proton temperature, and low proton  $\beta$ . The complex ejecta are not defined by these fields, but it is interesting to note that the averages for magnetic clouds (complex ejecta) are  $\langle B \rangle = 13 \pm 5$  nT ( $8 \pm 3$  nT),  $\langle T \rangle = 34,000 \pm 20,000$  °K ( $100,000 \pm 80,000$  °K), and  $\langle \beta \rangle = 0.06 \pm 0.04$  ( $0.25 \pm 0.09$ ).

All four of the fast magnetic clouds produced geomagnetic storms, but the forms of the disturbances measured by  $Dst$  varied depending on the relative contributions from the shocks, sheaths, and magnetic clouds, as one expects from many previous studies. Three of the fast complex ejecta produced no magnetic storms. Two complex ejecta produced geomagnetic storms, one by driving a shock into the rear of a magnetic cloud and the other by compressing southward magnetic fields in its leading edge and interaction region. The main bodies of fast complex ejecta are generally not very geoeffective, probably because the magnetic field direction is highly variable in them.

The solar activity associated with magnetic clouds was different from that associated with complex ejecta, insofar as we could determine within the limitations of the observations available. Most of the magnetic clouds were associated with single solar sources with several manifestations. These consisted of full halo CMEs associated at the surface with large, long-duration flares, disappearing filaments, coronal dimming regions, and coronal waves, all within  $25^\circ$  of geometrical Sun center. Most of the complex ejecta were associated with multiple (2–3) solar sources related to consisting of partial or full halo CMEs related to moderate flares with shorter durations than those associated with the magnetic clouds. About half of the complex ejecta also had clear DSF, dimming, and wave signatures. Thus the sources of complex ejecta tended to be of lower energy and complexity than the sources of magnetic clouds. This fact plus the interaction of multiple sources could account for the lack of coherent magnetic signatures in the complex ejecta.

All of the magnetic clouds were associated with an enhanced ratio  $O^{7+}/O^{6+} > 1$ , whereas only two of the complex ejecta had  $O^{7+}/O^{6+} > 1$ . Four of the complex ejecta had  $O^{7+}/O^{6+} > 0.7$ , but one did not. Thus the magnetic clouds were more strongly ionized than the complex ejecta in general. Neverthe-

less, all but one of the fast ejecta did have  $O^{7+}/O^{6+} > 0.7$  in at least part of the event.

Although most of the candidate source regions of complex ejecta were near Sun center, there was one notable exception. The complex ejection of event 7 was preceded by three candidate solar events: a DSF and X-ray loop arcade on January 19, 1999; an X-ray arcade and loop near an active region on January 20; and an energetic, long-duration limb flare later on January 20. This latter event would certainly have qualified as the source of the complex ejecta, except for its location near the limb. However, the Yohkoh Soft X-Ray Telescope (SXT) images showed an overall rapid expansion of loops to the south and well onto the disk from the flaring region. Thus it seems likely that at least the shock on January 22, 1999, was related to this explosion and possibly even the following ejecta. If this were the case, the ejecta signature might have been complex because only the flanks of a large event were intercepted by ACE at 1 AU. This would explain why the passage time of this ejection was anomalously short.

The consecutive magnetic cloud (event 2) and complex ejecta (event 5) shown in Figure 5 demonstrate clearly that magnetic clouds and complex ejecta can have different types of solar origins. Starting on April 29, 1998, a sequence of events originated from a single source region on the Sun. The first event was large, energetic, and near enough to Sun center that its western half (or part of it) traveled toward Earth. Yet it was isolated enough in time from the other events for its relatively simple shock-magnetic cloud ensemble to travel unimpeded from the Sun to 1 AU and be detected by ACE 2 days later. The source characteristics of this event were typical of such geoeffective structures: a halo CME associated at the surface with a flaring active region, an erupting filament, a large area of coronal dimming [Thompson *et al.*, 2000], and a coronal wave [Hudson *et al.*, 1998; Webb *et al.*, 2000a, 2000b, 2000c]. Then, starting on May 1, a series of similar solar eruptions, also aimed earthward, was followed by a “pileup” of material and tangled magnetic fields observed by ACE on May 4 and early May 5 as part of a complex ejection. This material was followed by several days of smoother ejecta likely coming from continuing eruptions of less energetic and less favorably aimed solar material.

## 9. Discussion of the Structure and Origin of Fast Complex Ejecta

We have shown that during the ascending phase of the present solar cycle, complex ejecta with disordered magnetic fields and fast speeds are present at 1 AU. Their rate of occurrence is of the same order as that of magnetic clouds. Significantly, their passage times and characteristic lengths are  $\sim 3$  times larger than those of the magnetic clouds in all except one case. Our results raise some fundamental questions. Why do fast complex ejecta exist? Why do most of the complex ejecta have much larger passage times than the magnetic clouds? Does the ratio of the number of fast complex ejecta to fast magnetic clouds vary with solar cycle? What are the structures and origins of complex ejecta?

The complex ejecta form a more heterogeneous class of objects than magnetic clouds. In what follows we consider some hypotheses concerning the structures and origins of complex ejecta. It is unlikely that one of these hypotheses describes all complex ejecta, and the list of hypotheses is not necessarily complete. Further studies are needed to determine definitively

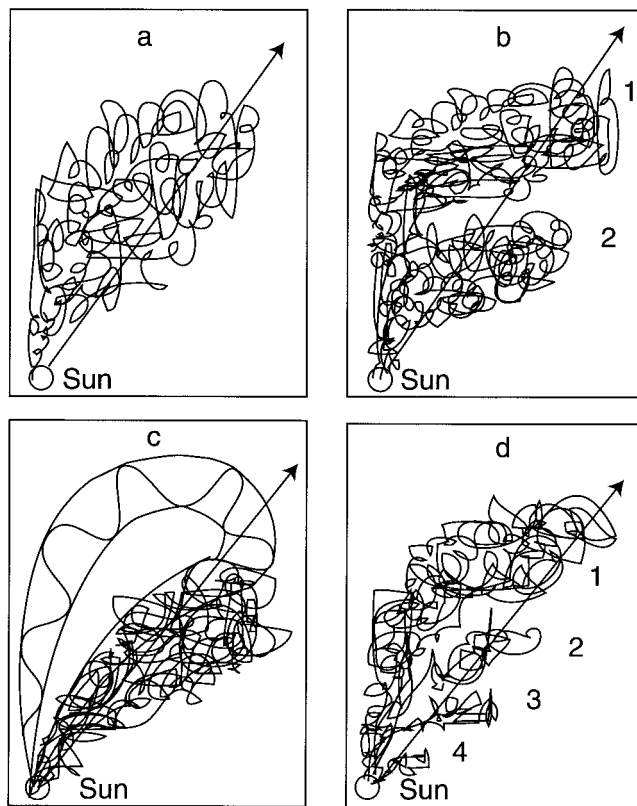


**Figure 13.** Hypothetical models of complex ejecta. (a) Complex ejecta with a relatively homogeneous structure produced by a single CME. (b) Complex ejecta produced by the interaction of two flows associated with two CMEs. (c) Complex ejecta overtaking and interacting with a magnetic cloud. (d) Complex ejecta produced by a series of mass ejections of various sizes.

the structure and origin of individual events. Comprehensive measurements of the composition of complex ejecta and associated solar phenomena are becoming available, and these together with theoretical studies should significantly improve our understanding of complex ejecta during the next few years. The purpose of this section is simply to summarize some of the possibilities and to stimulate further studies, rather than to provide definitive conclusions concerning the structure and origin of the individual complex ejecta presented in this paper.

The simplest hypothesis is that fast complex ejecta have the structure of a single object with tangled magnetic fields and originate from a single solar source, propagating without a qualitative change in form from the Sun to the Earth. This is essentially the picture proposed by Morrison [1956] as the cause of Forbush decreases. A schematic illustration of this model is shown in Figure 13a. The observed relatively large passage times of most complex ejecta at 1 AU cannot be produced by expansion of ejecta en route to Earth. However, it is possible that the sources of some complex ejecta persist longer than those of magnetic clouds. The complex ejection (event 9) in Figure 8, having a lengthy monotonically declining speed profile, was related to a single solar source and could conceivably be produced in this way. The complex ejection (event 6) in Figure 2 had a similar profile and is another candidate for an event produced by a persistent source.

Another hypothesis is that some complex ejecta are simply

crossings of a cocoon of tangled fields with a complex plasma structure that encloses a magnetic cloud that did not pass the spacecraft. This hypothesis is consistent with the observation that the passage time of the complex ejecta is larger than that of the magnetic cloud, but it requires special encounter geometry. Such cocoons do not surround some magnetic clouds, since one does not generally observe a region of tangled fields along a radial line in front of and behind them. However, it is possible that the small complex ejection (event 7) shown in Figure 6, which was associated with a limb flare on January 20, 1999, could represent the crossing of a cocoon of a magnetic cloud that was unobserved. Of course, a simpler interpretation is that the event was simply the crossing of the edge of a complex ejection such as that illustrated in Figure 13a. The unambiguous identification of a cocoon around a magnetic cloud requires multispacecraft data.

Two further hypotheses involve the possible transformation of magnetic clouds into complex ejecta and vice versa. On the one hand, it is conceivable that some complex ejecta originate in the corona as magnetic clouds, which become unstable and disordered. If this hypothesis is correct, one must explain why some complex ejecta can have high temperatures and lack strong magnetic fields and why complex ejecta can have larger passage times than magnetic clouds. On the other hand, it is conceivable that some CMEs produce complex ejecta near the Sun, which then relax to magnetic clouds via a process such as that embodied in Taylor's hypothesis. Such a transformation is observed in some laboratory experiments [Bellan, 2000] but has not been demonstrated in the solar wind. However, such a transformation would not explain the difference in the characteristic sizes of magnetic clouds and complex ejecta that we observe in most complex ejecta.

We know that fast complex ejecta and magnetic clouds can interact with one another, as illustrated schematically in Figure 13c. The May 1998 events in Figure 5 suggest such an interaction between a magnetic cloud (event 2) being overtaken by complex ejecta (event 5), and event 1 in Figure 3 might be interpreted in a similar way. Such interactions as well as further interactions with corotating streams give rise to complicated structures, which have been reviewed by Burlaga [1975, 1984, 1995]. Particular cases, based on multispacecraft observations, were discussed by Burlaga *et al.* [1987] and Behannon *et al.* [1991]. Burlaga *et al.* [1987] showed that many of the largest geomagnetic storms were produced by the high speeds and the amplification of magnetic fields by interacting ejecta. Understanding such complicated interactions will require more complete observations such as those that will be provided by Solar Terrestrial Relations Observatory (STEREO), Sentinel, and other missions, together with theoretical and modeling efforts.

A very plausible hypothesis concerning the structure and origin of some fast complex ejecta moving past Earth is that they are composed of two or more interacting flows from two or more sources. We have presented evidence based on solar data that most of the complex ejecta discussed in this paper could have been produced in this way. The observation of relatively large passage times for complex ejecta is a natural consequence of this hypothesis. The hypothesis is also consistent with recent LASCO coronagraph observations of series of CMEs and related smaller structures moving away from the Sun over the limb. There are several specific possibilities, and all are likely to be observed. The simplest possibility is that some complex ejecta represent a compound stream consisting

of two separate ejecta formed by the collision of two comparable CMEs, as illustrated in Figure 13b. Event 8 in Figure 7 might be an example of such complex ejecta. A second possibility is that a series of three or more CMEs from one or more regions on the Sun collide in the interplanetary medium and form complex ejecta with evolving structure, as illustrated in Figure 13d. We presented strong evidence from solar observations that such a series of ejections from the Sun could explain the complicated internal structure of the complex ejection (event 5) shown in Figure 5.

**Acknowledgments.** T.H.Z. and A.R. have been supported in part by NASA contracts NAG5-2810 and NAG5-7111.

Janet G. Luhmann thanks George Ho and Mark Popecki for their assistance in evaluating this paper.

## References

- Akasofu, S.-I., and S. Chapman, *Solar-Terrestrial Physics*, Oxford Univ. Press, New York, 1972.
- Baker, D. N., S.-I. Akasofu, W. Baumjohann, J. W. Bieber, D. H. Fairfield, E. J. Hones Jr., B. Mauk, R. L. McPherron, and T. E. Moore, Substorms in the magnetosphere, in *Solar Terrestrial Physics: Present and Future*, edited by D. M. Butler and K. Papadopoulos, *NASA Ref. Publ.*, 1120, 1984.
- Bame, S. J., A. J. Hundhausen, A. J. Asbridge, and I. B. Strong, Solar wind ion composition, *Phys. Rev. Lett.*, 20, 393–395, 1968.
- Bame, S. J., J. R. Asbridge, W. C. Feldman, J. T. Gosling, and R. D. Zwickl, Bi-directional streaming of solar wind electrons greater-than 80 eV—ISEE: Evidence for a closed-field structure within the driver gas of an interplanetary shock, *Geophys. Res. Lett.*, 8(2), 173–176, 1981.
- Behannon, K. W., L. F. Burlaga, and A. Hewish, Structure and evolution of compound streams at less than or equal to 1 AU, *J. Geophys. Res.*, 96, 21,213–21,225, 1991.
- Bellan, P. M., Simulating solar prominences in the laboratory, *Am. Sci.*, 88, 136–143, 2000.
- Buergi, A., and J. Geiss, Helium and minor ions in the corona and solar wind: Dynamics and charge states, *Sol. Phys.*, 103, 347–383, 1986.
- Burlaga, L. F., Interplanetary streams and their interaction with the Earth, *Space Sci. Rev.*, 17, 327–352, 1975.
- Burlaga, L. F., MHD processes in the outer heliosphere, *Space Sci. Rev.*, 39, 255–316, 1984.
- Burlaga, L. F., Magnetic Clouds, in *Physics of the Inner Heliosphere II*, edited by R. Schwenn and E. Marsch, pp. 1–19, Springer-Verlag, New York, 1991.
- Burlaga, L. F., *Interplanetary Magnetohydrodynamics*, Oxford Univ. Press, New York, 1995.
- Burlaga, L. F., E. Sittler, F. Mariani, and R. Schwenn, Magnetic loop behind an interplanetary shock: Voyager, Helios and IMP 8 observations, *J. Geophys. Res.*, 86, 6673–6684, 1981.
- Burlaga, L. F., K. W. Behannon, and L. W. Klein, Compound streams, magnetic clouds, and major geomagnetic storms, *J. Geophys. Res.*, 92, 5725–5734, 1987.
- Burlaga, L. F., R. Lepping, and J. A. Jones, Global configuration of a magnetic cloud, in *Physics of Magnetic Flux Ropes*, *Geophys. Monogr. Ser.*, vol. 58, edited by C. T. Russell, E. R. Priest, and L. C. Lee, pp. 343–364, AGU, Washington, D. C., 1990.
- Cane, H. V., I. G. Richardson, and T. T. von Rosenvinge, Cosmic ray decreases: 1964–1994, *J. Geophys. Res.*, 101, 21,561–21,572, 1996.
- Cane, H. V., I. G. Richardson, and G. Wibberenz, Helios 1 and 2 observations of particle decreases, ejecta, and magnetic clouds, *J. Geophys. Res.*, 102, 7075–7086, 1997.
- Cane, H. V., I. G. Richardson, and G. Wibberenz, Energetic particles and solar wind disturbances, *Space Sci. Rev.*, 87, 137–140, 1999.
- Chapman, S., *Solar Plasma, Geomagnetism and Aurora*, Gordon and Breach, Newark, N. J., 1964.
- Chapman, S., and J. Bartels, *Geomagnetism*, Oxford Univ. Press, New York, 1940.
- Cocconi, G., K. Greisen, P. Morrison, T. Gold, and S. Hayakawa, The cosmic ray flare effect, *Nuovo Cimento Suppl. Ser. X*, 8(2), 161–168, 1958.

- Crooker, N. U., and E. W. Cliver, Postmodern view of M-regions, *J. Geophys. Res.*, **99**, 23,383–23,390, 1994.
- Dungey, J. W., Interplanetary magnetic field and the auroral zones, *Phys. Rev. Lett.*, **6**, 47, 1961.
- Geiss, J., et al., The southern high-speed stream: Results from the SWICS instrument on Ulysses, *Science*, **268**(5213), 1033–1036, 1995.
- Gloeckler, G., et al., Investigation of the composition of solar and interstellar matter using solar wind and pickup ion measurements with SWICS and SWIMS on the ACE spacecraft, *Space Sci. Rev.*, **86**, 495, 1998.
- Gloeckler, G., L. A. Fisk, S. Hefti, N. A. Schwadron, T. H. Zurbuchen, F. M. Ipavich, J. Geiss, P. Bochsler, and R. F. Wimmer-Schweingruber, Unusual composition of the solar wind in the 2–3 May 1998 CME observed with SWICS on ACE, *Geophys. Res. Lett.*, **26**(2), 157–160, 1999.
- Gosling, J. T., Coronal mass ejections and magnetic flux ropes in interplanetary space, in *Physics of Magnetic Flux Ropes*, *Geophys. Monogr. Ser.*, vol. 58, edited by C. T. Russell, E. R. Priest, and L. C. Lee, pp. 343–364, AGU, Washington, D. C., 1990.
- Gosling, J. T., Coronal mass ejections: An overview, in *Coronal Mass Ejections*, *Geophys. Monogr. Ser.*, vol. 99, edited by N. Crooker, J. A. Joselyn, and J. Feynman, pp. 9–16, AGU, Washington, D. C., 1997.
- Gosling, J. T., V. J. Pizzo, and S. J. Bame, Anomalously low proton temperatures in the solar wind following interplanetary shock waves: Evidence for magnetic bottles?, *J. Geophys. Res.*, **78**, 2001–2009, 1973.
- Gosling, J. T., D. N. Baker, S. J. Bame, W. Feldman, and R. D. Zwickl, Bidirectional solar wind electron heat flux events, *J. Geophys. Res.*, **92**, 8519–8535, 1987.
- Gosling, J. T., S. J. Bame, D. J. McComas, and J. L. Phillips, Coronal mass ejections and large geomagnetic storms, *Geophys. Res. Lett.*, **17**(7), 901–904, 1990.
- Gosling, J. T., D. J. McComas, J. L. Phillips, and S. J. Bame, Counterstreaming solar wind halo electron events: Solar-cycle variations, *J. Geophys. Res.*, **97**, 6531–6535, 1992.
- Hefti, S., H. Grunwaldt, P. Bochsler, and M. R. Aellig, Oxygen freeze-in temperatures measured with SOHO/CELIAS/CTOF, *J. Geophys. Res.*, **105**, 10,527–10,536, 2000.
- Henke, T., J. Woch, U. Mall, S. Livi, B. Wilken, R. Schwenn, G. Gloeckler, R. von Steiger, R. J. Forsyth, and A. Balogh, Differences in the O7+/O6+ ratio of magnetic cloud and non-cloud coronal mass ejections, *Geophys. Res. Lett.*, **25**(18), 3465–3468, 1998.
- Hirshberg, J., S. J. Bame, and E. E. Robbins, Solar flares and helium enrichments, *Sol. Phys.*, **23**, 467, 1972.
- Ho, G. C., D. C. Hamilton, G. Gloeckler, and P. Bochsler, Enhanced solar wind  $^3\text{He}^{2+}$  associated with coronal mass ejections, *Geophys. Res. Lett.*, **27**(3), 309–312, 2000.
- Hudson, H. S., J. R. Lemen, O. C. St. Cyr, A. C. Sterling, and D. F. Webb, X-ray coronal changes during halo CMEs, *Geophys. Res. Lett.*, **25**(14), 2481–2484, 1998.
- Hundhausen, A. J., Ionization state of the interplanetary plasma, *J. Geophys. Res.*, **75**, 5485–5496, 1968.
- Hundhausen, A. J., *Coronal Expansion and Solar Wind*, Springer-Verlag, New York, 1972.
- Hundhausen, A. J., H. E. Gilbert, and S. Bame, The state of ionization of oxygen in the solar wind, *Astrophys. J.*, **152**, L3–L5, 1968.
- Klein, L. W., and L. F. Burlaga, Interplanetary magnetic clouds at 1 AU, *J. Geophys. Res.*, **87**, 613–624, 1982.
- Larson, D. E., et al., Tracing the topology of the October 18–20, 1995, magnetic cloud with 0.1–10(2) keV electrons, *Geophys. Res. Lett.*, **24**(15), 1911–1914, 1997.
- Lepping, R. P., J. A. Jones, and L. F. Burlaga, Magnetic field structure of interplanetary magnetic clouds at 1 AU, *J. Geophys. Res.*, **95**, 11,957–11,965, 1990.
- Lindeman, F. A., Note on the theory of magnetic storms, *Philos. Mag.*, **38**, 669, 1919.
- Marsden, R. G., T. R. Sanderson, C. Tranquille, K.-P. Wenzel, and E. J. Smith, ISEE 3 observations of low-energy proton bidirectional events and their relation to isolated interplanetary magnetic structures, *J. Geophys. Res.*, **92**, 11,009–11,019, 1987.
- Montgomery, M. D., J. R. Asbridge, S. J. Bame, and W. Feldman, Solar wind electron temperature depressions following some interplanetary shock waves: Evidence for magnetic merging, *J. Geophys. Res.*, **79**, 3103–3110, 1974.
- Morrison, P., Solar origin of cosmic ray time variations, *Phys. Rev.*, **101**, 1397, 1956.
- Neugebauer, M., and R. Goldstein, Particle and field signatures of coronal mass ejections in the solar wind, in *Coronal Mass Ejections*, *Geophys. Monogr. Ser.*, vol. 99, edited by N. Crooker, J. A. Joselyn, and J. Feynman, pp. 245–251, AGU, Washington, D. C., 1997.
- Neukomm, R. O., and P. Bochsler, Diagnostics of closed magnetic structures in the solar corona using charge states of helium and of minor ions, *Astrophys. J.*, **465**(1), 462–472, 1996.
- Newton, H. W., Solar flares and magnetic storms, *Mon. Not. R. Astron. Soc.*, **103**, 244, 1943.
- Osherovich, V., and L. F. Burlaga, Magnetic clouds, in *Coronal Mass Ejections*, *Geophys. Monogr. Ser.*, vol. 99, edited by N. Crooker, J. A. Joselyn, and J. Feynman, pp. 157–168, AGU, Washington, D. C., 1997.
- Owociki, S. P., and J. D. Scudder, The effect of a non-Maxwellian electron-distribution on oxygen and iron ionization balances in the solar corona, *Astrophys. J.*, **270**(2), 758–768, 1983.
- Palmer, I. D., F. R. Allum, and S. Singer, Bidirectional anisotropies in solar cosmic ray events: Evidence for magnetic bottles, *J. Geophys. Res.*, **83**, 75–90, 1978.
- Richardson, I. G., and H. V. Cane, Regions of abnormally low proton temperature in the solar-wind (1965–1991) and their association with ejecta, *J. Geophys. Res.*, **100**, 23,397–23,412, 1995.
- Richardson, I. G., and D. V. Reames, Bidirectional  $\sim$  MeV/amu ion intervals in 1973–1991 observed by the Goddard Space Flight Center Instruments on IMP-8 and ISEE-3/ICE, *Astrophys. J. Suppl. Ser.*, **85**, 411–432, 1993.
- Richardson, I. G., C. J. Farrugia, and H. V. Cane, A statistical study of the behavior of the electron temperature in ejecta, *J. Geophys. Res.*, **102**, 4691–4699, 1997.
- Richardson, I. G., V. M. Dvornikov, V. E. Sdobnov, and H. V. Cane, Bidirectional particle flows at cosmic ray and lower (similar to 1 MeV) energies and their association with interplanetary coronal mass ejections/ejecta, *J. Geophys. Res.*, **105**, 12,579–12,591, 2000.
- Sanderson, T. R., R. G. Marsden, R. Reinhard, K.-P. Wenzel, and E. J. Smith, Correlated particle and magnetic field observations of a large scale magnetic loop structure behind an interplanetary shock, *Geophys. Res. Lett.*, **10**(9), 916–919, 1983.
- Sanderson, T. R., R. Reinhard, P. van Nes, and K.-P. Wenzel, Observations of three-dimensional anisotropies of 35–1000 keV protons associated with interplanetary shocks, *J. Geophys. Res.*, **90**, 19–27, 1985.
- Shodhan, S., N. Crooker, S. Kahler, R. J. Fitzenreiter, D. E. Larson, R. P. Lepping, G. L. Siscoe, and J. T. Gosling, Counterstreaming electrons in magnetic clouds, *J. Geophys. Res.*, **105**, 27,261–27,268, 2000.
- Skoug, R. M., et al., A prolonged  $\text{He}^+$  enhancement within a coronal mass ejection in the solar wind, *Geophys. Res. Lett.*, **26**(2), 161–164, 1999.
- St. Cyr, O. C., et al., Properties of coronal mass ejections: SOHO LASCO observations from January 1996 to June 1998, *J. Geophys. Res.*, **105**, 18,169–18,185, 2000.
- Thompson, B. J., E. W. Cliver, N. Nitta, C. Delannée, and J. P. Delaboudinière, Coronal dimmings and energetic CMEs in April–May 1998, *Geophys. Res. Lett.*, **27**(10), 1431–1434, 2000.
- Tsurutani, B. T., W. D. Gonzalez, F. Tang, S. I. Akasofu, and E. J. Smith, Origin of interplanetary southward magnetic fields responsible for major magnetic storms near solar maximum (1978–1979), *J. Geophys. Res.*, **93**, 8519–8531, 1988.
- Wang, H., et al., Comparison of the April 29, 1998 M6.8 and November 5, 1998 M8.4 flares, *Astrophys. J.*, **536**, 971–981, 2000.
- Webb, D., B. Jackson, P. Hick, R. Schwenn, V. Bothmer, and D. Reames, Comparison of CMEs, magnetic clouds, and bidirectionally streaming proton events in the heliosphere using Helios data, *Adv. Space Res.*, **13**(9), 71–74, 1993.
- Webb, D. F., R. P. Lepping, L. F. Burlaga, C. E. DeForest, D. E. Larson, S. F. Martin, S. P. Plunkett, and D. M. Rust, The origin and development of the May 1997 magnetic cloud, *J. Geophys. Res.*, **105**, 27,251–27,259, 2000a.
- Webb, D. F., E. W. Cliver, N. U. Crooker, O. C. St. Cyr, and B. J. Thompson, Relationship of halo coronal mass ejections, magnetic clouds, and magnetic storms, *J. Geophys. Res.*, **105**, 7491–7508, 2000b.
- Webb, D. F., R. P. Lepping, N. U. Crooker, S. P. Plunkett, and O. C. St. Cyr, Studying CMEs using LASCO and in-situ observations of halo events, *Bull. Am. Astron. Soc.*, **32**, 825, 2000c.
- Wysocki, F. J., J. C. Fernandez, I. Henins, T. R. Jarboe, and G. L.

- Marklin, Evidence for a pressure-driven instability in the CTX spheromak, *Phys. Rev. Lett.*, *61*, 2457, 1988.
- Zhang, G., and L. F. Burlaga, Magnetic clouds, geomagnetic disturbances, and cosmic ray decreases, *J. Geophys. Res.*, *93*, 2511–2518, 1988.
- Zurbuchen, T. H., S. Hefti, L. A. Fisk, G. Gloeckler, and N. A. Schwadron, Magnetic structure of the slow solar wind: Constraints from composition data, *J. Geophys. Res.*, *105*, 18,327–18,336, 2000.
- Zwickl, R. D., J. R. Asbridge, S. J. Bame, W. C. Feldman, J. T. Gosling, and E. J. Smith, Plasma properties of driver gas following interplanetary shocks observed by ISEE-3, in *Solar Wind Five*, edited by M. Neugebauer, *NASA Conf. Publ.*, 2280, 711–717, 1983.
- A. Reinard and T. H. Zurbuchen, Dept. of Atmospheric, Oceanic, and Space Sciences, University of Michigan, Ann Arbor, MI 48109.
- R. M. Skoug, Los Alamos National Laboratory, Los Alamos, NM 87545.
- C. W. Smith, Bartol Research Institute, University of Delaware, Newark, DE 19711.
- D. F. Webb, Institute for Scientific Research, Boston College, Chestnut Hill, MA 02167.

---

L. F. Burlaga, Laboratory for Extraterrestrial Physics, NASA Goddard Space Flight Center, Greenbelt, MD 20771. (burlaga@lepvax.gsfc.nasa.gov)

(Received June 30, 2000; revised October 10, 2000; accepted October 10, 2000.)

